https://doi.org/10.15407/ufm.25.01.074

M.G. BOLOTOV*, G.P. BOLOTOV, and M.M. RUDENKO*****
Chernihiv Polytechnic National University,
95 Shevchenko Str., UA-14035, Chernihiv, Ukraine
* bolotovmg@gmail.com, ** bolotovgp@gmail.com, *** rudenko_bear@ukr.net

THE IMPACT OF NITRIDING PARAMETERS ON EVOLUTION OF PROPERTIES OF STAINLESS-STEEL SURFACE PLASMA-NITRIDED IN GLOW DISCHARGE

Plasma nitriding in a glow discharge is a relatively new and extremely promising method of steel surface hardening. Ion-nitrided samples show a tendency to a longer lifespan during severe wear and cyclic loading compared to the traditional gas nitriding. However, a significant disadvantage of plasma thermochemical processes is their relatively long duration of about 20–30 hours. As a result, the surface treatment becomes inefficient and too expensive. As known, the properties of the nitrided layer, its phase composition and growth rate depend strongly on the parameters of the plasma nitriding (temperature, time, gas pressure, composition of the gas mixture, *etc.*). At the same time, there is still an open question regarding the choice of optimal modes of hardly-nitrided stainless-steels plasma nitriding, which will ensure of high treatment efficiency and obtaining of high-hardness strengthened layers with a controlled structural–phase composition. As established, to prevent the formation of Cr–N metastable phases' precipitations on the surface of stainless steels, the appearance of which leads to deterioration of their corrosion performance, the treating temperatures should be limited: ≤450 °C. Low-temperature plasma nitriding provides the formation of a homogeneous nitrided layer of 'white' phase with a nitrogen concentration of 15 at.% and more. This phase ensures the nitrided-surface hardness of 1500 *HV*, which is by 4-to-5 times greater than the hardness of the untreated one. The possibility of the plasma-nitriding intensification by increasing the gas pressure in the reactor in the range from 130 to 400 Pa is shown. This provides an increase in the thickness of the nitrided layer and its

Citation: M.G. Bolotov, G.P. Bolotov, and M.M. Rudenko, The Impact of Nitriding Parameters on Evolution of Properties of Stainless-Steel Surface Plasma-Nitrided in Glow Discharge, *Progress in Physics of Metals*, **25**, No. 1: 74–113 (2024)

hardness from ≈8 μm up to ≈18 μm and ≈700 *HV* up to ≈1500 *HV*, accordingly. Significant growth dynamics of the nitrided layer on the stainless-steels' surfaces is achieved by determining the optimal 3-component gas mixture with a content of 55% Ar–30% N_2–15% H_2 that ensures the obtaining of a hardened layer with a thickness of ≈30 μm and a surface hardness of 1100 *HV*.

Keywords: glow discharge, plasma nitriding, thermochemical treatment, ion surface modification, stainless steels.

1. Introduction

Stainless steels are multicomponent systems, mainly Fe–Cr–C or Fe–Cr–Ni, which possess high resistance against general or local types of corrosion. The high corrosion resistance of these steels is due to the presence of a chemically resistant chromium oxide film on their surfaces, which has the ability to regenerate after mechanical damage, protecting the alloy from the harmful environmental effect [1, 2]. However, stainless steels have received limited application in the field of mechanical engineering and many others, in which the main requirements are high surface hardness, fatigue and wear resistance. Even in case of high-strength martensitic stainless steel, in order to increase the wear resistance of its surface under conditions of severe wear and cyclic loadings the surface-hardening treatment is strongly recommended, if high corrosion resistance remains the main criterion [3].

In order to improve the strength and tribological properties of machine parts, the methods of their modification by applying strengthening protective coatings by chemical (CVD) or physical (PVD) vapour deposition, as well as methods of thermochemical treatment (TCT) are widely used [4].

The practice of industrial application has shown that among the existing methods, the combination of chemical exposure and thermally activated diffusion of atoms of alloying elements, during TCT, improves the mechanical properties of steel surfaces, ensuring the reliability and durability of machine parts. Particularly, plasma nitriding in a glow discharge is one of the most effective methods of increasing surface hardness, wear and corrosion resistance of steels. Compared to the conventional gas nitriding, plasma surface treatment, where the sample's surface affected by the ions of the saturation element accelerated in a high-tension electric field, provides the number of crucial advantages. First and foremost, it enables effective depassivation (activation) of the samples surface, creating conditions for the free nitrogen diffusion into the metal [5]. Secondly, ion bombardment creates on the treated surface a large number of crystal lattice defects (vacancies, dislocations, *etc.*) to a depth of up to 50 μm, intensifying plasma nitriding due to radiation-stimulated diffusion [6].

Thus, the effectiveness of plasma nitriding will be determined by the rate of nitrogen diffusion in the metal volume, the intensification of which is associated with the solution of the main problem — the long nitriding duration. The issue of controlling the phase composition and the properties of the modified layers is closely related to the effectiveness of plasma nitriding as well. Since, as is known, the presence of alloying elements in the stainless steels' composition, in particular nitrides forming, affects significantly the hardening characteristics, morphology and kinetics of the nitrided surface formation. For instance, at the typical nitriding temperatures, chromium has a greater tendency to form CrN rather than a solid solution with iron [7]. The formed new phase will serve as the energy barrier for nitrogen atoms diffusion deep into the steel samples preventing formation of strengthening layer. In order to prevent of such phases' formation, the plasma nitriding parameters strict controlling (temperature, time, gas pressure, composition of the gas mixture, *etc.*) is quite crucial. At the same time, the process of ion-plasma nitriding is multifactorial, the technological factors of which are in a complex and, at times, insufficiently studied dependence.

In this regard, the issue of establishing the regularities of the course of diffusion processes and the kinetics of the superhard strengthening phase formation during glow discharge plasma nitriding of stainless steels in order to ensure of high treatment efficiency is extremely relevant.

2. The Role of Glow Discharge Plasma for Nitriding Process of Stainless Steels

For a high-quality industrial application of the plasma nitriding process, it is necessary to provide a deeper understanding of the mechanism of interaction between plasma particles and the treating surface.

According to Ref. [8], the simplest way of glow discharge initialization is to apply a voltage of 300–1100 V to the electrodes placed into vacuum chamber which filled with the required gas medium and pumped down to the certain gas pressure (133–1330 Pa for plasma nitriding). As a result of discharge gap breakdown, over time an abnormal glow discharge is established, in which the entire cathode surface is uniformly covered with a glow. When implementing such a (diode) glow discharge scheme, the treating parts serve as a cathode simultaneously. Under these conditions, cleaning (activation) of the cathode, heating and further saturation with the nitrogen atoms will occur due to the bombardment of its surface with ions of the working gas, accelerated in the region of the cathode potential drop [9].

The modern theory of interaction mechanism of the gas-discharge medium with the metal cathode (the treated samples) during plasma nitriding in the glow discharge is characterized by two main approaches. The

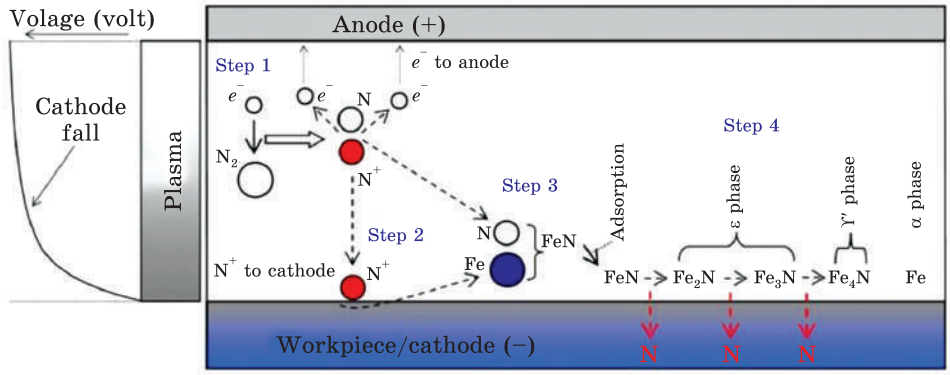

Fig. 1. The main physicochemical interactions of glow discharge plasma with the treated surface [14]

basis of the first model, formulated by the authors of Refs. [10–12], is the effect of iron sputtering from the cathode surface as a result of ion bombardment. This theory underlies the modern understanding of the mechanism of diffusion saturation of steels with nitrogen in glow discharge plasma. In this case, FeN iron nitrides formed in the near-cathode region as a result of the interaction of sputtered iron atoms with the ionized nitrogen start to move toward the cathode. Adsorbing on the samples surface, FeN transforms gradually into the ε-phase (ε-$Fe_{2-3}N$) and the γ′-phase (γ′-Fe_4N), forming compound layer. The atomic nitrogen released because of such reaction creates a solid solution of α_N, α'_N or γ_N, namely, the phases of expanded by nitrogen ferrite, martensite or austenite, accordingly (depending on the class of steel), that diffuse deep into the surface forming a diffusion zone [13]. Together, the compound and diffusion zones create so-called 'white' layer of internal nitriding. These are exactly the phases, which recognized as providing of high hardness and wear resistance of the treated surface. Figure 1 illustrates the formulated principle.

The core of the second model, which was shown in Ref. [15], is the assumption that the intensification of nitrogen diffusion in steel is not as much the effect of the physical cathode sputtering as the number of structural and surface imperfections formed due to ion bombardment and the density of nitrogen ions near the samples surface, accordingly. Formed defects, in their opinion, serve as easy ways of nitrogen diffusion in steel. Thus, the authors of Ref. [16] conducted research on the conditions of dislocations formation and their movement because of ion bombardment. After analysing the obtained results, they concluded that the direction of dislocations movement due to the ion bombardment of the treated surface coincides directly with the way of diffusion flow of saturation element. The latter is proven by the results of many metallographic and x-ray studies.

However, no matter how significantly these theories differ, in our opinion, they have one common ground related to the atomic nitrogen diffusional mass transfer deep into the treated surface as a consequence of its bombardment with the ions of working gas active component. Thus, the diffusion of saturation elements deep into the strengthened metal body is a defining process for all known methods of thermochemical treatment, and the intensification of its rate is the main way of the treatment process improvement in general.

In accordance with Fick's first law Ref. [17, 18], the diffusion flow of saturation elements J is determined by the diffusing atoms concentration gradient and the diffusion coefficient D, accordingly, and can be found by the next expression:

$$J = -D\left(\frac{dn}{dz}\right), \tag{1}$$

where n is the concentration of atoms of the saturation element, z is the co-ordinate calculated normally to the saturation surface.

In turn, the diffusion coefficient is defined as

$$D = D_0 \exp\left(-\frac{E_a}{RT}\right); \tag{2}$$

here, E_a is the activation energy of the diffusion process (the minimum energy that must be imparted to an atom to transfer it from one equilibrium state to another); T is the temperature of the treated surface; R is an universal gas constant; D_0 is the value that characterizes the frequency of collisions of reacting molecules (in the theory of active collisions, it has a certain dependence on temperature). In Ref. [19], it is shown that temperature changes in the range of 200–300 °C leads to a change in D_0 by 10%.

Analysing Eqs. (1) and (2), we can conclude that an increase in the diffusion flow density (J) can be achieved by increasing the treating temperature, or by applying treatment reducing the diffusion activation energy (E_a). Thus, the authors of Ref. [20] note that the use of TCT where the ions or electrons affect surface of the treated samples, the facilitation of saturation atoms diffusion occurs mainly due to the generation of surface and structural defects that reduce E_a, *i.e.*, because of radiation stimulated diffusion [21]. At the same time, the chemical, adsorption and catalytic activity of the surface layers changes significantly, which also favourably affects the treatment quality. The authors of Ref. [22] observe a significant increase in the diffusion mobility of atomic nitrogen on the surfaces of stainless steels 20Cr13 and 40Cr13, plasma nitrided in glow discharge, with the increasing in nitriding temperature and the concentration of the defects generated on the treated surface. In Ref. [23] on the study of low-energy implantation with ni-

trogen ions and ion nitriding of 20Cr13 steel, the authors indicate that an increase in the depth of the hardened layer alongside with the nitrides volume fraction can be achieved by diffusion of nitrogen atoms through the structural defects: dislocations, grain and subgrain boundaries. The authors of Ref. [24] experimentally demonstrated the effectiveness of ion pre-treatment of Fe–0.32Mn–1.8Cr–0.2Mo–0.98Al–0.37C steel before low-temperature plasma nitriding. In their work, they note the appearance of nanostructured nitrides layer, increasing significantly the hardness and wear resistance of steel during plasma nitriding is a glow discharge at a temperature of 400 °C. The formation of such a structure closely associated with the creation on the treated surface of a large number of defects (grain boundaries and dislocations) as a result of ion pre-treatment. These defects, in turn, create so-called nitride forming 'traps' increasing significantly of nitrogen atomic diffusion and facilitate the nitriding process generally.

Thus, glow discharge plasma plays a substantial role in the thermochemical treatment processes creating the number of a complex plasma–surface physical and chemical processes that can be described as follow.

1. An inelastic collision of fast electrons, emitted from the cathode surface because of ion bombardment, with the gaseous atoms and molecules resulting in their ionization. This creates the conditions for the formation of an active environment saturated with atomic nitrogen ions near the cathode surface.

2. Ion bombardment of the cathode surface inevitably leads to the formation of a large number of surface and structural defects, intensifying of nitrogen diffusion deep into the treated sample.

3. Cathode sputtering, which is also a consequence of ion bombardment, creates the conditions for removing of natural oxides from the treated surface before nitriding, preventing of its reappearance during nitriding process as well. This is essential for free atomic nitrogen diffusion into the depth of treated samples.

4. Cathode heating to the treating temperatures by converting of ions' kinetic energy into thermal one, while the ion bombardment of nitrided surface.

The above processes are closely intertwined and their unhindered flow ensures a high rate of nitrogen diffusion saturation, thus the application of nitrided surface with the required structure, mechanical and tribological properties. Normally, these processes control is provided by changing of plasma nitriding main parameters, such as: temperature, treatment time, the composition of the gas mixture and the gas pressure in the reactor. However, the listed parameters are closely related and have a complex effect on the plasma nitriding efficiency. In this regard, the comprehensive analysis of such impact will be considered down the paper.

3. The Impact of Treatment Temperature and Time on the Kinetics of Nitrided Layers Formation on the Surface of Stainless Steels at the Glow Discharge Plasma Nitriding

As it was already shown, the diffusion rate of saturation atoms during plasma nitriding will be determined by the process temperature. Since, as is known, after implantation in the surface layers, further nitrogen diffusion deep into the sample occurs mainly due to thermally activated diffusion. Therefore, the intensification of atomic nitrogen diffusion mass transfer will take place with increasing of treatment temperature.

At the same time, in the prevalent majority of works [25–30] it is noted a certain threshold temperature for plasma nitriding of stainless steels, exceeding of which inevitably leads to the decomposition of iron–nitrogen solid solution with the α-ferrite formation and according precipitation of CrN. Such a decomposition with a subsequent increase in the surface hardness results simultaneously in a dramatic decrease in the corrosion resistance of steel due to the depletion of Cr from the metal matrix.

A known work Ref. [31] on the study of the influence of plasma nitriding temperature and time on the corrosion performance of AISI 316L austenitic and AISI 470 superferritic stainless steels in a glow discharge. The experiments carried out in a gas mixture of 25% H_2–75% N_2 at a pressure of 300 Pa and voltages of 300–400 V. The chemical composition of steels is given in Table 1.

Table 1. **Chemical composition (%) of AISI 470 and AISI 316L steels [31]**

Steel	C	Si	Mn	Cr	Mo	Ni	Ti	Nb
AISI 470	0.01	0.35	0.19	24.3	0.04	0.24	0.13	0.2–0.3
AISI 316L	0.03	1.0	2.0	16–18	2–3	10–14	–	0.2

Table 2. **Results of experimental studies of the effect of nitriding temperature and time on the thickness of the hardened layer obtained on AISI 470 and AISI 316L steels [31]**

Temperature, °C	Steel	Treatment time, h	Thickness, μm
520	AISI 316L	2	26.20 ± 1.15
		4	41.60 ± 1.56
		6	54.70 ± 2.02
	AISI 420	2	27.20 ± 1.44
		4	40.05 ± 1.58
		6	54.40 ± 1.78
400	AISI 316L	4	4.07 ± 0.18
	AISI 420	4	6.72 ± 0.37

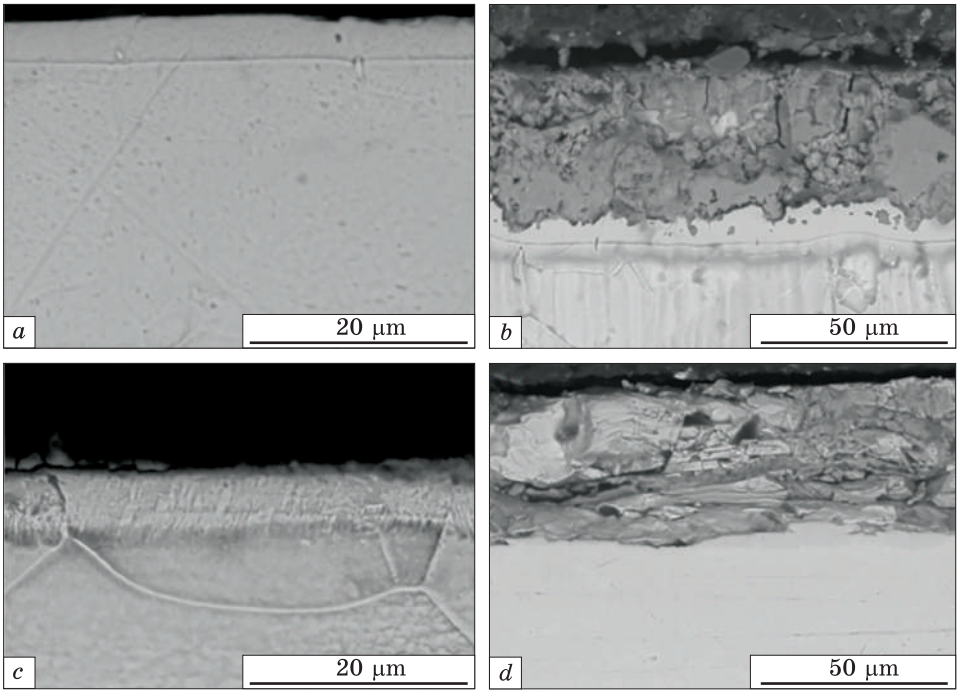

Fig. 2. Microstructure of the nitrided layer obtained on AISI 316L (*a*, *c*) and AISI 470 (*b*, *d*) at 400 °C (*a*, *b*) and 520 °C (*c*, *d*) for 4 hours [31]

Research was conducted on samples measuring 30×20×10 mm. Two temperature modes were investigated: (1) T = 520 °C, where the treatment time varied in the range of 2–6 h; (2) T = 400 °C, where the nitriding time was fixed at the level of 4 h.

Analysing the obtained results, shown in Table 2, the authors note that an increase in both nitriding temperature and time leads to an increase in the thickness of the hardened layer. Moreover, the influence of nitriding temperature on the formation and growth of the nitrided layer is much more significant than the heat exposure time. Thus, the increasing of treatment temperature from 400 °C to 520 °C, in their experiments, led to an increase in the thickness of the nitrided layer obtained on AISI 316L and AISI 470 steels, from ≈4 μm to ≈41 μm and from ≈6 μm to ≈40 μm, respectively. While increasing the nitriding time from 2 to 6 hours, at the maximum saturation temperature of 520 °C, led to an increase in the thickness of the nitrided layer from ≈26 μm to ≈54 μm and from ≈27 μm to ≈54 μm for AISI 316L and AISI 470, respectively.

At the same time, analysing cross-section photomicrographs of nitrided samples shown in Fig. 2, the authors note a dramatic violation of the nitrided layers homogeneity obtained on both steels at a temperature of 520 °C.

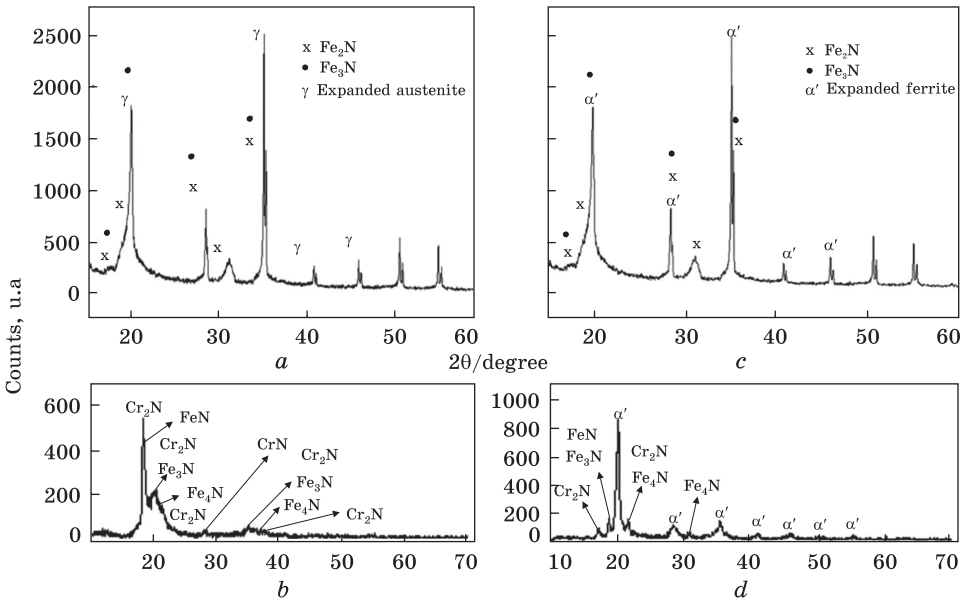

Fig. 3. X-ray diffraction patterns of plasma nitrided AISI 316L and AISI 470 samples at 400 °C (*a*, *c*) and 520 °C (*b*, *d*) for 4 hours [31]

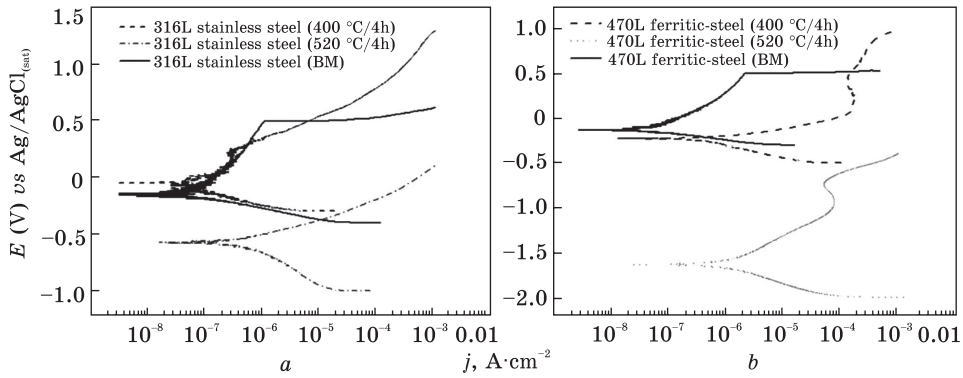

Fig. 4. Potentiodynamic polarization curves for austenitic AISI 316L (*a*) and superferritic AISI 470 (*b*) stainless steels [31]

The x-ray diffraction (XRD) patterns of plasma-nitrided AISI 316L and AISI 470 samples are presented in Fig. 3. They show that the nitrided layer consists mainly of an iron nitrides FeN, Fe_3N, Fe_4N, and chromium nitrides CrN and Cr_2N compound layer. While the structure of samples nitrided at a temperature of 400 °C consists of expanded austenite (γ_N) and expanded ferrite (α_N) phases for AISI 316L and AISI 470 steels, respectively. However, the authors point out the low treatment dynamics under these conditions.

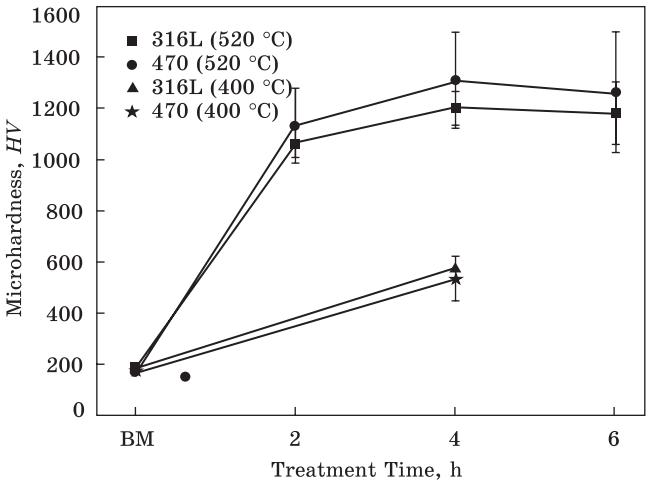

Fig. 5. Microhardness of AISI 316L and AISI 470 steels surfaces nitrided at 400 °C and 520 °C as a function of treatment time [31]

The obtained results correlate with those ones represented in Ref. [32] on the study of the temperature influence on the characteristics of the nitrided layer obtained on austenitic AISI 316 and superaustenitic S31254 (X1CrNiMoCuN20-18-7) stainless steels. The nitriding process was conducted in a gas mixture of 80% H_2–20% N_2 at pressures gas 500 Pa during 5 hours. The temperature was varied from 400 up to 500 °C in steps of 50 °C. Like previous researchers, the authors note the formation of a homogeneous nitrided layer, consisting mainly of γ_N-phase at a nitriding temperature of 400 °C, with a total thickness of 4 μm for both steels. At the same time, at a treating temperature of 500 °C, the authors point out the heterogeneous nitrided layer formation (mainly iron and chromium nitride phases) with a thickness of 22 and 26 μm for AISI 316 and S31254, respectively. The CrN precipitation on the plasma treated steels the authors observed at a temperature of about 450 °C.

The results of corrosion tests are shown in Fig. 4. Analysing the obtained potentiodynamic polarization curves, the authors [31] note higher anodic currents on steels nitrided at a temperature of 520 °C that indicates deterioration in a corrosion performance of treated samples.

The dependences of the nitrided surface hardness on the treatment time are shown in Fig. 5. The obtained curves indicate that with an increase in the nitriding time up to 4 hours at a temperature of 520 °C, the microhardness of nitrided surface of AISI 316L and AISI 470 steels reached of 1306 and 1196 *HV*, respectively. The further treatment time increasing up to 6 hours, the curves stabilize at the previous level. The authors explain such behaviour by a decrease in the total nitrogen concentration on the surface of the samples due to their diffusion deep into the substrate. The latter leads to an increase in the length of the diffu-

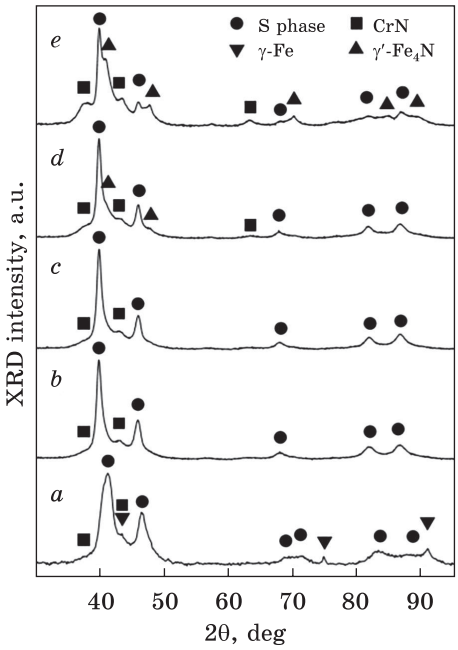

Fig. 6. X-ray diffraction patterns of AISI 316L steel samples nitrided at different temperatures: 673 K (*a*), 703 K (*b*), 723 K (*c*), 743 K (*d*), and 773 K (*e*) [33]

sion zone with stabilization of the surface microhardness. It would be interesting to see the distribution of microhardness along the depth of the hardened layer. However, the authors do not provide such results.

At the same time, at a nitriding temperature of 400 °C on AISI 316L and AISI 470 steels, it is possible to obtain a layer with a hardness of 572 and 534 *HV*, respectively, against 183 *HV* and 166 *HV* on the reference (untreated) sample.

The work Ref. [33] gives the results of studies of the treatment temperature impact on the structure and surface properties of AISI 316L stainless steel plasma nitrided in a DC glow discharge. Nitriding was carried out in a gas mixture of 80% N_2–20% H_2 at a pressure in the reactor of 1000 Pa for 5 hours. The 40×18×4 mm samples were ground and polished using 6 μm diamond suspension to reduce the surface roughness to 0.3 μm. The nitriding temperature varied from 673 K (400 °C) to 773 K (500 °C). Analysing the obtained results shown in Table 3, the authors also note an increase in the thickness of nitrided layer from 4 to 47 μm with an increase in the treatment temperature from 673 to 773 K.

The XRD patterns of AISI 316L steel, nitrided at different temperatures, are shown in Fig. 6. X-ray analysis of the nitrided samples phase composition showed the presence of expanded austenite γ_N-phase (or *S*-phase) in all modified samples. Thus, the samples nitrided at a temperature of 673 K (400 °C) are mainly made up of *S*-phase. With increasing of nitriding temperature up to 723 K (450 °C), small amount

Table 3. **Thickness of the hardened layer obtained on AISI 316L stainless steel nitrided at different temperatures [33]**

Nitriding temperature, K	The thickness of nitrided layer, μm	Nitriding temperature, K	The thickness of nitrided layer, μm
673	4 ± 1	743	18 ± 2
703	10 ± 1	773	47 ± 3
723	13 ± 1		

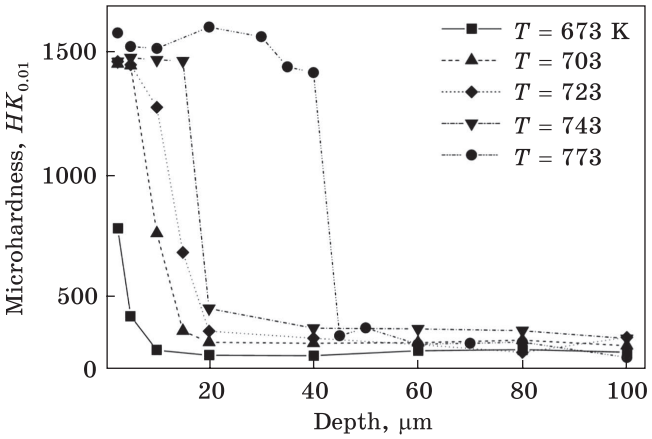

Fig. 7. Knoop microhardness profiles of AISI 316L nitrided sample at 673 K (*a*), 703 K (*b*), 723 K (*c*), 743 K (*d*), and 773 K (*e*) [33]

of CrN precipitates appear along with the S-phase, the number of which rises with increasing of treatment tempera-ture. The authors also note an increase in the amount of Cr, Mo, Mn, and Si along with a decrease in the concentration of nickel and iron in the modified layer of the sample nitrided at a temperature of 723 K.

The x-ray analysis showed that in the hardened layer of samples nitrided at a temperature of 773 K (500 °C), the phases of CrN and Fe_4N alongside with the γ_N-phase are also observed. At the same time, there is a dramatic increase in the concentration of Cr and Mo with a corresponding decrease in the concentration of Ni and Fe compared to the reference composition.

The hardness depth profiles of the nitrided samples shown in Fig. 7. The authors point out that all modified samples have a high surface hardness with a sharp decrease through the depth to the microhardness value of untreated sample. As expected, sam-ples nitrided at a temperature of 673 K show the lowest value of microhardness, which, according to the authors, is due to the small thickness of the hardened layer. The samples modified at tempera-tures of 703–743 K show approximately the same value of micro-hardness at the level of 1450 $HK_{0.01}$, which corresponds to micro-hardness of γ_NN-phase of expanded austenite. The further enhance-ment in the microhardness of the samples up to ≈1550 $HK_{0.01}$, along with an increase in temperature to 773 K, authors attribute to the rising role of solid nitride precipitates.

Also known work Ref. [34] on the study of the impact of nitriding temperature and time on the surface properties of austenitic stainless steel alloy A286/AISI 660 (15% Cr, 26% Ni, 2.23% Ti, 0.24% Al, 0.31% V). Before nitriding, the samples were heated to an austenizing temperature of 900–1010 °C, followed by annealing at a temperature of 720 °C for 16 hours. The plasma nitriding was carried out in a DC abnormal glow discharge in a gas mixture of 25% N_2–75% H_2 at pressures in the

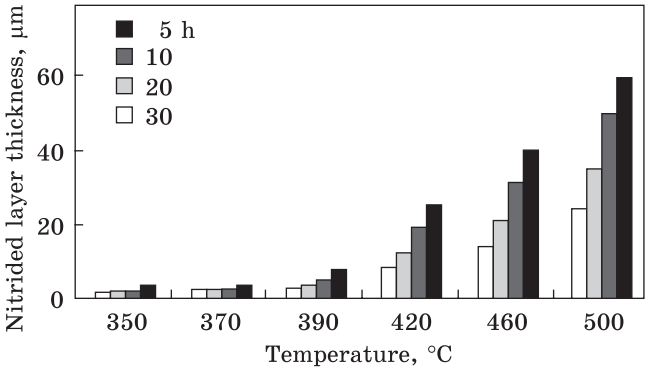

Fig. 8. Thickness of modified layers of A286 steel as a function of nitriding temperature and time [34]

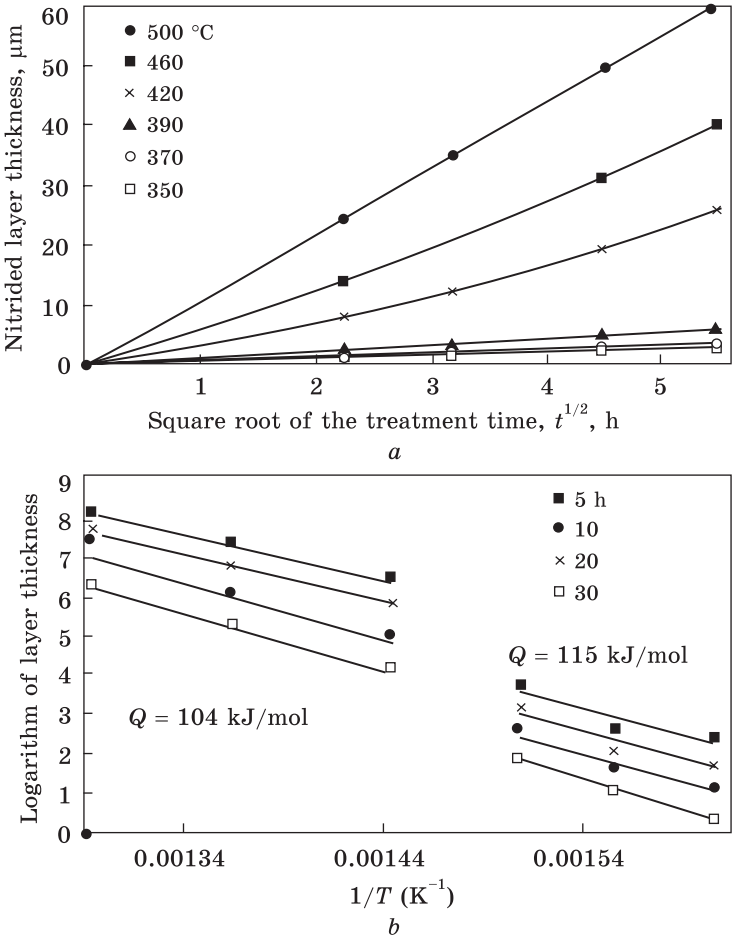

Fig. 9. The effect of nitriding time (*a*) and temperature (*b*) on the kinetics of hardened layers formation on A286 stainless steel [34]

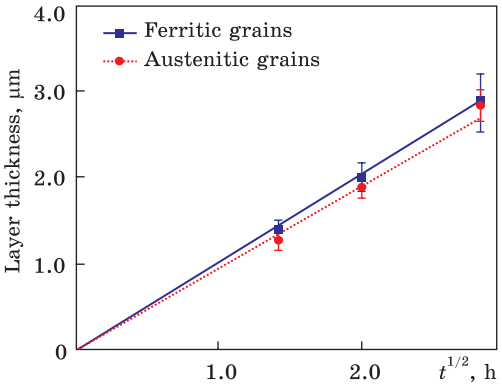

Fig. 10. The nitrided layer thickness as a function of the square root on the nitriding time for a layer formed on austenite and ferrite grains of UNS s32750 steel [35]

temperature varied from 350 to 500 °C, while the treating time was 5, 10, 20, and 30 h.

The authors present the results of the research in form of histo-gram shown in Fig. 8. Analysing the obtained results, the authors point out that rather nitriding temperature affects the growth rate of the modified layer then treatment time. In their research, the changing of treatment temperature from 350 up to 500 °C resulted in the growth of nitrided layer thickness by more than 10 times, whilst the increasing of treatment time from 5 to 30 hours led to a far less significant effect.

The obtained results allowed the authors of Ref. [34] to study the growth kinetics of A286 steel nitrided layers. Thus, they have come to a two extremely vital conclusions. Primarily, they deter-mined that at a constant treatment temperature, the thickness of the nitrided layers is proportional to the square root of the treat-ment time (Fig. 9, *a*). This is fully consistent with the theory of the growth of the nitrided layer due to the nitrogen diffusional penetration into the sample. Secondly, the authors have found that the dependence of the nitrided layers thickness on the treatment temperature has two ranges (Fig. 9, *b*). The mechanisms operating in these ranges may vary significantly. The transition from the slow growth of the modified layer to intensive one plays an im-portant role in determining the nitriding kinetics of austenitic stainless steel.

The influence of nitriding duration on the structure and properties of the modified layers obtained on the super duplex stainless steel UNS S32750 (25.6% Cr, 6.8% Ni and 4.1% Mo) was separately studied in [35]. A main feature of duplex stainless steels is the ex-istence of a two-phase ferrite-austenite microstructure with a per-centage ratio $\alpha:\gamma$ of 50:50. There is an assumption that nitriding of such steels leads to the simultaneous formation of γ_N-expanded austenite and α_N-expanded ferrite phases [36, 37].

The samples measuring $20\times20\times3$ mm were previously polished and grounded with 1 μm abrasive suspension Al_2O_3 and 1 μm dia-mond paste in order to obtain a mirror surface. Directly in the re-actor, the samples were sputter-cleaned in a glow discharge at a voltage of 700 V for 30 min at a temperature about 300 °C. Nitrid-ing was carried out in a pulsed DC glow discharge with a pulse frequency of 4.16 kHz in the gas mixture of 70% N_2 + 20% H_2 + 10% Ar at pressures of 400 Pa. The nit-

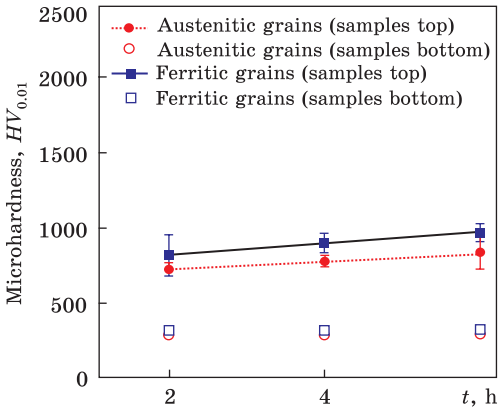

Fig. 11. Microhardness profiles of the surfaces of UNS s32750 steel nitrided at a temperature of 350 °C during of 2, 4, and 8 hours [35]

riding temperature was fixed at 350 °C, while the nitriding time was 2, 4, and 8 hours. As in previous review, the authors have also noted the linear depend-ence of the nitrided layer thickness on the square root of the treatment time (Fig. 10), which confirms the theory of diffusion-controlled nitrogen mass transfer deep into the treated surface.

Analysing the graph, the authors concluded that the nitrided layer formation begins already at the initial stage of ion activation of the surface. This indicates the removal of a natural oxide layer from the treated surface, serving as a barrier for nitrogen diffu-sional penetration.

X-ray diffraction patterns show, that under the given condi-tions, the appearance of a single-phase structure with γ_N-phase on the surface of UNS s32750 steel is observed without any evidences of α_N-expanded ferrite. The authors explain this effect by the fact that nitrogen is a strong austenite stabilizer and the substitutional diffusion, during which the interaction of ferrite with nitrogen at-oms with the γ_N-phase formation at these temperatures is possible, is actually frozen.

Microhardness profiles of nitrided samples of UNS s32750 steel at different treatment time are shown in Fig. 11. The authors observe a simultaneous increase in surface microhardness on both austenitic and ferritic grains with an increase in the nitriding duration. Thus, in their experiments, on the samples nitrided at exposure duration of 2, 4, and 8 hours, the value of surface microhardness was 811, 893, and 968 $HV_{0.01}$ for ferrite grains and 727, 775, and 833 $HV_{0.01}$ for austenite grains, respectively.

In Ref. [38], the influence of nitriding duration on the properties of modified layers of AISI 316L steel was specifically investigated. The samples preparation and actual nitriding were carried out under the same conditions as given above in Ref. [33]. The nitriding temperature was ensured at the level of 703 K (430 °C), the treatment time was 1, 2, 3.5, and 5 hours. The properties of the nitrided layers and their phase composition were compared with the original (untreated) sample of AISI 316L steel.

Analysing the phase composition of samples nitrided at different treating time, the authors note, that the main phase of all treated samples is γ_N-phase of expanded austenite. The thickness of hardened layer

gone up from 4 to 10 μm with increasing nitriding duration from 1 to 5 hours. It should be noted that untreated sample also had signs of a nitrided phase about 3 μm thick. As in the previous case, the authors associate this effect with a certain penetration of atomic nitrogen ions into the surface layer of the original sample at the stage of ion activation because of reverse cathode sputtering.

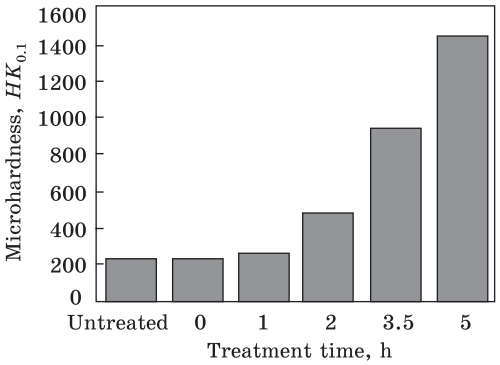

Fig. 12. Microhardness of nitrided AISI 316L steel layers vs. the nitriding duration [38]

The microhardness values of the nitrided samples show a significant strengthening of the modified layer in comparison with the untreated one. Thus, the microhardness of nitrided surfaces increased from 220 $HK_{0.1}$ up to ≈1450 $HK_{0.1}$ with an increase in treatment time from 1 to 5 hours (Fig. 12). The authors attribute an increase dramatically in the microhardness of nitrided layers to a growth in their thickness because of treatment time increasing.

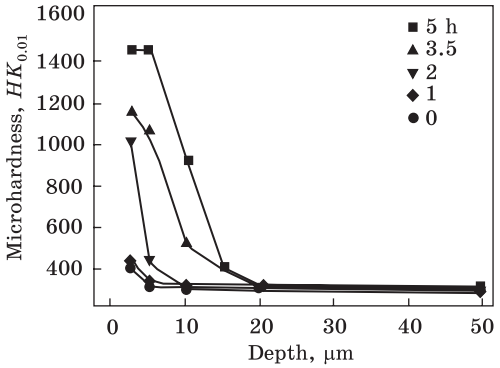

Fig. 13. Microhardness profiles of 316L samples plasma nitrided at different treatment times [38]

In Figure 13, the microhardness profiles of AISI 316L steel nitrided samples are shown. As seen, the distribution of microhardness along the thickness of the sample has a classical feature for this treating method, with a maximum in the surface vicinity and a sharp decrease to the microhardness value of untreated sample as it moves deeper.

In Ref. [39], the influence of nitriding temperature on the properties and formation kinetics of modified layers on AISI 420 (Fe–0.40C–13.5Cr–0.25V) martensitic stainless steel was investigated. The samples were pre-quenched in oil at an austenisation temperature of 1025 °C followed by double tempering at a temperature of 580 °C. Just before nitriding, the samples were subjected to the cathode sputtering in dense H_2 plasma in order to remove the passivating oxide layer from the surface of the samples. Plasma nitriding was carried out in anomalous DC glow discharge at a treatment temperature changes in the range from 480 to 560 °C with a step of 20 °C for 4 hours in a gas mixture

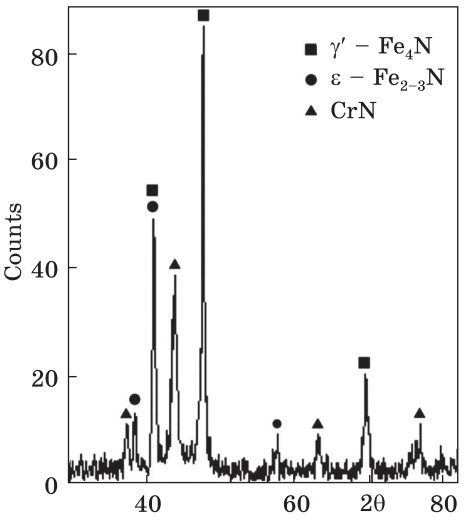

Fig. 14. X-ray diffraction patterns of AISI 420 steel nitrided at 560 °C [39]

$N_2:H_2$ = 3:1 at a pressure in the reactor of 250 Pa.

Cross-section photomicrographs of samples nitrided at temperatures of 480 and 560 °C show, that under such conditions a heterogeneous nitrided layer consisting of a compound and diffusion layers is formed. According to the authors, this is because of large percentage of nitrogen in the gas mixture. At the same time, the authors of Ref. [40] managed to avoid the compound layer formation on AISI 440B steel (0.90% C–18% Cr) at a nitriding temperature of 520 °C for 4 hours in a gas mixture of 50% of N_2.

Instead, the authors of Ref. [41, 42] note that in order to obtain a homogenous nitrided layer on AISI 410 and AISI 420 steels, consisting mainly of the α'_N-phase of expanded martensite, the low-temperature plasma nitriding should be applied.

The XRD pattern of nitrided samples at a temperature of 560 °C are presented in Fig. 14 show the predominant presence of iron (γ′-Fe_4N, ε-$Fe_{2-3}N$) and chromium (CrN) nitrides.

Microhardness profiles of nitrided at different temperatures samples of AISI 420 are shown in Fig. 15. The graph demonstrates a strengthening effect dramatically from the precipitation of the nitride phase, both iron and chromium, in the nitrided layer. The authors have also noted that all modified samples have a high surface hardness of 1570 $HV_{0.025}$ compared to the untreated one (400 $HV_{0.025}$).

Knowing the penetration depth of nitrogen atoms in samples treated at different temperatures, the authors find the nitrogen diffusion coefficient using the following expression:

$$X = \sqrt{D_N t}\,, \tag{3}$$

where X is the length (depth) of diffusion, D_N is an effective nitrogen diffusion coefficient, and t is a nitriding time.

Using expressions (2) and (3), the authors calculated the diffusion coefficient $D_0 = 6.066 \cdot 10^{-5}$ cm^2/s and the activation energy E_a = = 125.13 kJ/mol^{-1} = 1.295 eV for AISI 420 steel. They note that the calculated diffusion coefficient is as a result of both volume nitrogen

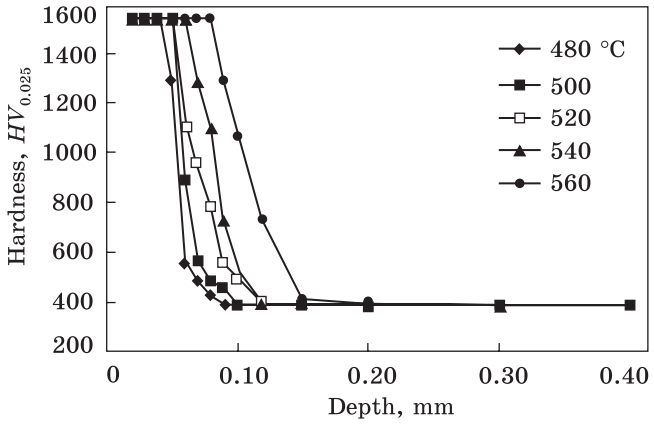

Fig. 15. Microhardness profiles of AISI 420 samples nitrided at different temperatures [39]

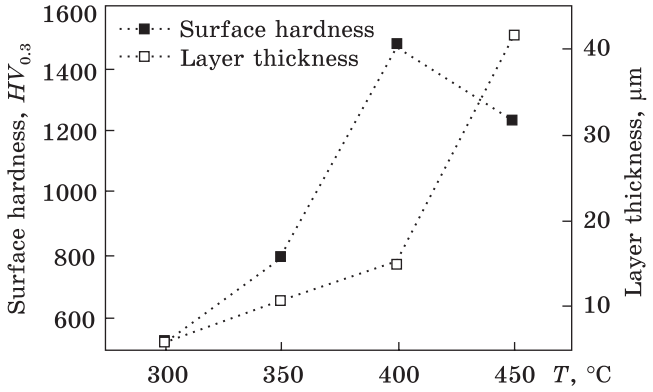

Fig. 16. The thickness and microhardness of AISI 420 nitrided layer *vs*. the treatment temperature [44]

diffusion and the reaction of nitrides deposition. This caused a high-calculated activation energy outnumbering two times the E_a for pure iron and four times for AISI 420 itself.

As is known from the literature Ref. [43], due to the high density of crystal defects formed because of hardening, the diffusion rate of atoms in martensitic stainless steels is slightly higher rather than in austenitic ones. However, as in the case of austenitic steels, there is also a need to limit the treatment temperature in order to prevent harmful precipitation of chromium nitrides along the grain boundaries.

In Ref. [44], investigating the effect of the plasma nitriding parameters on the surface properties of AISI 420 martensitic stainless steel, the authors indicate the feasibility of treating at a temperature not exceeding 400 °C. The study was carried out in a gas mixture of 70% N_2 — 20% H_2 — 10% Ar at a pressure in the working chamber of 400 Pa. The voltage on the electrodes was fixed at 600 V. The effect of temperature on the properties of the nitrided surface was evaluated by varying from 300 to 450 °C with a step of 50 °C in a constant time of 6 h. The inf-

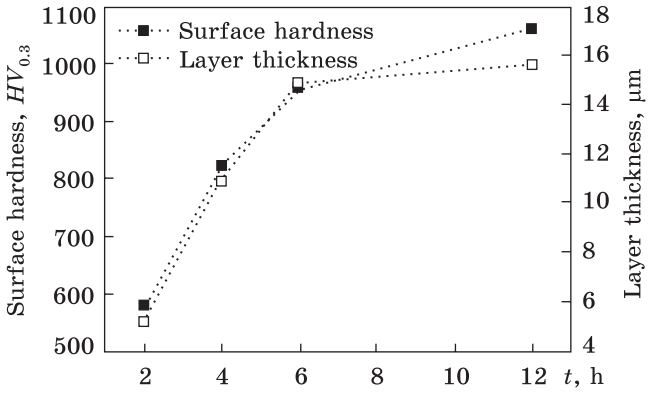

Fig. 17. The thickness and microhardness of hardened layer on AISI 420 steel nitrided at a temperature of 350 °C *vs.* the nitriding time [44]

luence of the treatment time was studied at a nitriding temperature of 350 °C, while the nitriding time varied within 2, 4, 6, and 12 h.

In Figure 16, the thickness and hardness of plasma nitrided surface layer on AISI 420 as a function of temperature is presented. The authors point out the parabolic nature in the thickness of nitrided layer while increasing temperature, with a maximum of 43 μm at a temperature of 450 °C. In contrast, the surface microhardness of the nitrided layer changes in extremal law with a maximum of 1500 *HV* at a treating temperature of 400 °C.

The decrease in the samples microhardness amid rising nitrided layer thickness at temperatures above 400 °C the authors attribute to the negative effect of CrN resulting in α'_N-phase decreasing. However, this opinion contrasts with the results presented above. In Figure 17, the dependences of the thickness and microhardness of AISI 420 steel modified layers at a temperature of 350 °C on nitriding time is also presented.

The experimentally obtained results show the increasing both the thickness and hardness of the modified surfaces with an increase in the treating time from 2 to 12 h.

The authors of Ref. [45, 46] indicated the expediency of AISI 410 and AISI 420 steels plasma nitriding at temperatures not exceeding of 400 °C. They have also noted that the nitriding at temperatures ≈400 °C prevents the precipitation both CrN as well as ε and γ′-iron nitrides, which is also undesirable.

According to Ref. [47], the formation of iron nitrides (ε-$Fe_{2-3}N$ and γ′-Fe_4N) on nitrided surfaces of martensitic stainless steels, leads to significant internal stresses along the grain boundaries, increasing the diffusion layer fragility. This effect is mainly due to the difference in iron nitride's elementary structure and the crystal structure of the steel itself. For example, in Ref. [48], after nitriding AISI 420 steels at a temperature of 480 °C, the appearance of delayed cracks in the nitrided

layer after a 24-month incubation period without any external disturbances is noted.

Thus, with an increase in the nitriding temperature, there is a general tendency to increase of the nitrided layer thickness. At the same time, the microhardness can decrease at high nitriding temperatures because of α'_N- or γ_N-phase decomposition. Moreover, at high-temperature nitriding, there is a decrease in the corrosion resistance of stainless steels due to the depletion of the metal matrix by chromium because of CrN phase precipitation. In this regard, in order to intensify of stainless steels plasma nitriding, the increase in the treating temperature is not effective at all. On the contrary, in order to prevent the harmful phases precipitation, that increase the diffusion activation energy blocking of nitrogen diffusion mass transfer deep into the samples, the nitriding temperature must be strictly limited. Under such conditions, for obtaining of 'white' layer without harmful phases with a thickness that will ensure of high surface hardness, the nitriding duration should be tens of hours.

4. Influence of the Pressure and Gas Composition on the Kinetics of Hardened Layers Formation on Stainless-Steel Surfaces Nitrided in a Glow Discharge

Among other plasma nitriding technological parameters, the ion composition of the nitrogen-containing gas medium and the gas pressure in the reactor should be highlighted. As is known, the ion flow density of any component of the gas mixture will depend on its percentage and the gas pressure in the reactor. Meanwhile, the energy of the ions will be determined by the mass of the particles falling on the cathode and the voltage at the discharge electrodes, accordingly.

It is clear that, in nitriding processes (both gas and plasma ones), the main source of saturation atoms is nitrogen. However, the other components are also presented in the gas mixture. See, for example Refs. [49–52], addition of hydrogen to the gas mixture allows to create a reducing plasma environment, increasing its ability to remove oxides. Finally, the addition of argon increases the heating and sputtering rate of the cathode, without noticeable chemical reactions on the treated surface [53].

Sometimes, instead of N_2 — H_2 or N_2 — Ar gas mixture, ammonia is also used [54–57], the molecules of which are dissociated in the plasma into nitrogen and hydrogen atoms. The use of NH_3 somewhat simplifies of plasma nitriding process control, but creates environmental problems [58].

In turn, the gas pressure during plasma nitriding will depend on the method of the gas discharge plasma excitation and, as a rule, are limited to the conditions of the glow discharge stable existence. It is known from the literature [21] that during conventional plasma nitriding (using

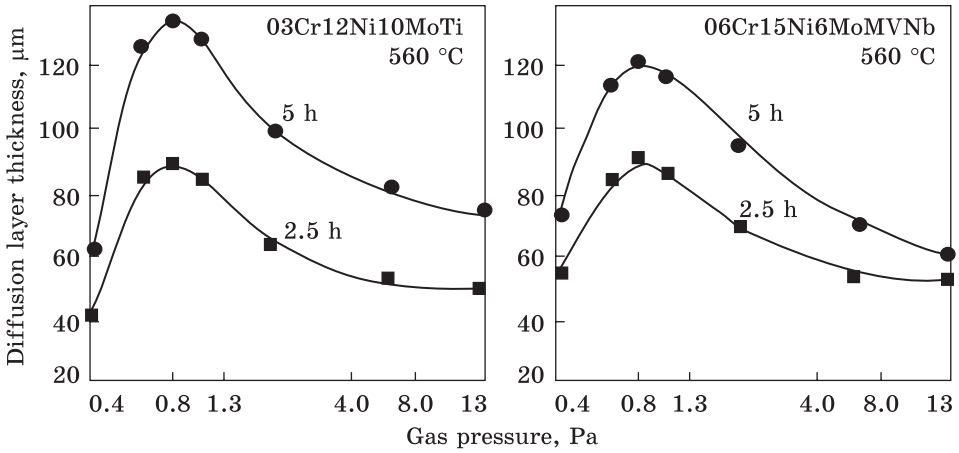

Fig. 18. Effect of nitrogen pressure on the diffusion layer thickness at the plasma nitriding of 03Cr12Ni10MoTi and 06Cr15Ni6MoWVNb steels [21]

abnormal DC glow discharge), working pressures vary in the range from 133 Pa to 1330 Pa. At a gas pressure below the threshold, where the glow discharge excitation is still possible, the energy of the ions is insufficient for treated surface heating to nitriding temperatures. In turn, plasma nitriding at pressures exceeding the upper limit of 1330 Pa is complicated by partial or complete loss of glow discharge stability and its transition into an electric arc. The latter, as shown in [59–63], leads to violation of nitriding process modes and, as a result, undesirable overheating and melting of the treating surfaces.

On the other hand, as is known from the gas discharge theory [64], the lower the gas pressure within the reactor, the greater the free path length of the particles. Therefore, the atomic nitrogen ions should reach the treated surface with greater energy. With an increase in the gas pressure in the reactor, along with a general tendency to decrease of nitrogen ions kinetic energy, the dense plasma formation on the treated surfaces with a higher concentration of atomic nitrogen is observed. The authors of Ref. [65] report that, under such conditions, an increase in the number of reactive nitrogen atoms penetrating into the sample and, as a result, a decrease in the nitriding duration is observed. However, such an effect, most likely, is of an extreme nature. Thus, the authors of Ref. [21] report a decrease in the concentration of atomic nitrogen ions with an excessive increase in gas pressure. This theory is also confirmed by the results of experimental studies given in [66] dedicated to the plasma nitriding of 03Cr12Ni10MoTi and 06Cr15Ni6MoWVNb martensitic stainless steels. The research was conducted in a pure nitrogen environment (100% N_2) at a temperature of 560 °C for 2.5 and 5 h. The obtained results are presented in Fig. 18.

Analysing the obtained results, the authors concluded that under such conditions there is a certain pressure that ensures maximum saturation of the samples surface (the largest diffusion layer thickness), exceeding of which leads to a decrease in the nitriding efficiency. The authors attribute this to a decrease in the effect of cathode and reverse cathode sputtering with increasing of nitrogen pressure in the working chamber. This leads to an increase in the thickness of the outer nitrides saturated layer (more likely with CrN), *i.e.*, an increase in its barrier effect on nitrogen diffusion deep into the sample. At the same time, at the maximum saturation pressure and nitriding temperature of 560 °C, within 5 hours, the authors reported obtaining a modified layer with a thickness of 120 μm.

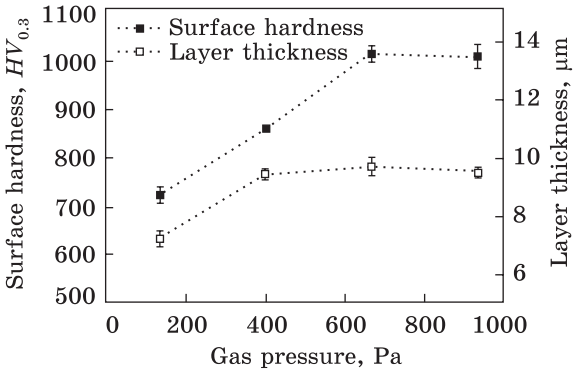

Fig. 19. Dependence of the thickness and hardness of the nitrided layer on AISI 420 at 350 °C for 6 hours at different gas pressures [44]

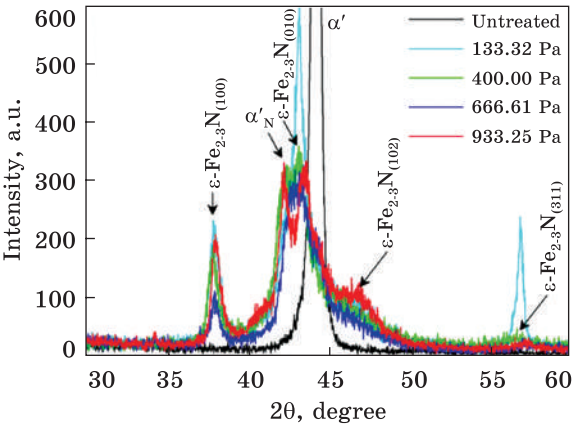

Fig. 20. X-ray diffraction patterns of AISI 420 steel samples plasma nitrided at 350 °C for 6 hours with different gas pressures [44]

The hardness of such a layer was 1000 $HV_{0.05}$. The authors note that it took approximately 12 hours to obtain the same thickness of the nitrogen-saturated layer in an ammonia environment.

In contrast, in Ref. [44] the authors report the growth of the nitrided layer thickness on AISI 420 steel from 7 to 9.5 μm with an increase in gas pressure from 133.3 Pa (1 Torr) to 400 Pa (3 Torr). When the gas pressure in the reactor is further increased up to 933.3 Pa (7 Torr), the thickness of the nitrided layer remains practically unchanged. Meanwhile, the hardness of the nitrided surface increases from 730 to 1050 *HV* with the rising of the gas pressure to 666.6 Pa (5 Torr) and stabilizes at this level with the further pressure increasing up to 933.3 Pa (Fig. 19). The research was conducted at a temperature of 350 °C for 6 hours in

an environment of 70% N_2–20% H_2–10% Ar. The authors also associate the decline of both the nitrided layer growth intensity and its hardness with the loss of nitrogen ions energy due to a decrease in their free path length when the pressure goes up.

The XRD patterns of hardened layer on AISI 420 steel samples nitrided at different gas pressures are shown in Fig. 20. The authors note that nitrided layer of all treated samples are mainly made up of ε-phase of iron nitrides $Fe_{2-3}N$ and the α'_N-phase of expanded martensite.

In Ref. [67], the impact of the gas pressure on the structure and properties of AISI-316L steel nitrided samples was investigated. Plasma nitriding was carried out at a temperature of 430 °C for 5 hours in a gas mixture of 80% N_2–20% H_2 at vary in a gas pressure ranging from 150 to 2000 Pa. The obtained results along with the nitriding parameters are given in Table 4.

The authors note the predominant presence of γ_N-phase with the nitride's precipitation in the hardened layers' structure depended on the gas pressure in the reactor. Thus, the authors observe a significant amount of the nitrides phase (both iron γ'-Fe_4N and chromium CrN nitrides) already at pressures of 250 Pa. With a further increase in the gas pressure up to 500 Pa, a certain decrease in the nitrides phase was observed. Barely noticeable precipitation of CrN was occurring at a pressure of 1000 Pa.

In their experiments, the increasing of a gas pressure from 150 to 250 Pa resulted in a slight increase in the nitrided layer thickness from 15 to 18 μm. With a further increase in gas pressure up to 2000 Pa, the thickness of the nitrided layer decreased by half and was 9 μm. This totally correlates with the results shown in Ref. [66] and gave the authors a ground to consider a pressure of 250 Pa as the one that provides maximum nitrogen saturation.

The authors attribute the decline in microhardness from 1540 to 1286 *HK* with an increase in a gas pressure from 150 to 2000 Pa to the rising role of surface nitride precipitates. As was already mentioned, they act as blockers of the atomic nitrogen diffusion into the samples surface layers.

Table 4. **Plasma nitriding parameters, the thickness of the nitrided layers and it's microhardness on AISI-316L steel samples, treated at different gas pressures [67]**

Gas pressure, Pa	Current density, mA/cm^2	Voltage drop, V	The thickness of nitride layer, μm	Knoop microhardness, $HK_{0.05}$
150	1.2	290	15	1540
250	1.5	225	18	1506
500	2.1	180	12	1405
1000	2.6	175	10	1272
2000	2.7	195	9	1286

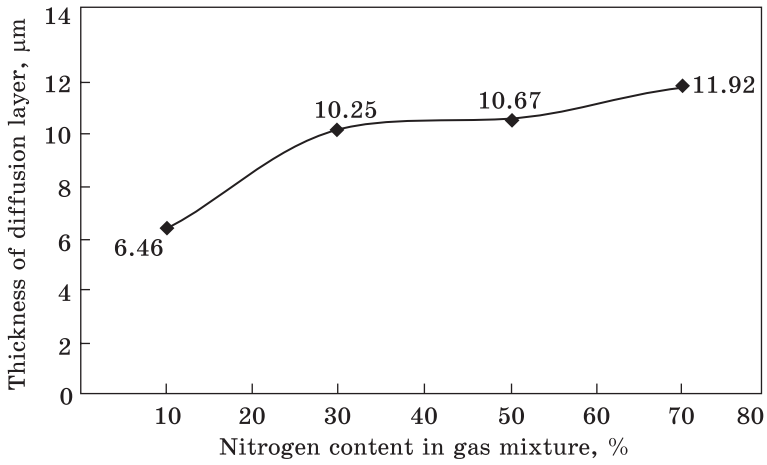

Fig. 21. Effect of the gas mixture on the thickness of the nitrided layer on AISI 304 steel [76]

The authors of Refs. [68, 69] report an increase in the modified layer thickness on AISI 304 steel when the gas pressure in the reactor is reduced from 400 to 130 Pa, as well as significant decline in the nitriding efficiency at pressures below 400 Pa. A significant growth of the nitrogen saturated layer on samples of AISI 316L and AISI 202 steels at a treatment temperature of 400 °C with a decrease in gas pressure from 500 to 130 Pa is also reported in Ref. [70].

As already mentioned, the gas mixture composition effects dramatically the glow discharge plasma properties therefore, the structural and mechanical characteristics of plasma nitrided layers. During plasma nitriding, treated samples interact with plasma particles, where nitrogen is a crucial component. However, pure nitrogen discharge plasma sources (100% N_2) haven't found the wide industrial application because they cannot provide the necessary tribological and mechanical characteristics of the surface [71–73]. Moreover, the authors of Refs. [74, 75] report the decrease in corrosion resistance of plasma nitrided stainless steels with an excessive increase in nitrogen content in N_2:H_2 gas mixture because of CrN precipitation.

Thus, the work of Ref. [76] reports on the nitrogen total concentration in modified layers does not exceed of 13% with the rising of N_2 content in nitrogen-hydrogen gas mixture from 10% to 70% during plasma nitriding of AISI 304 (X5CrNi18-10) steel. Instead, the thickness of the nitrided layer almost doubled from 6.46 to 11.92 μm (Fig. 21). It should be noted that the research was conducted at fixed temperature of 450 °C, gas pressure of 400 Pa, and nitriding time of 6 hours. Four variants of the gas mixture were studied: (1) 10% N_2–90% H_2; (2) 30% N_2–70% H_2; (3) 50% N_2–50% H_2; (4) 70% N_2–30% H_2.

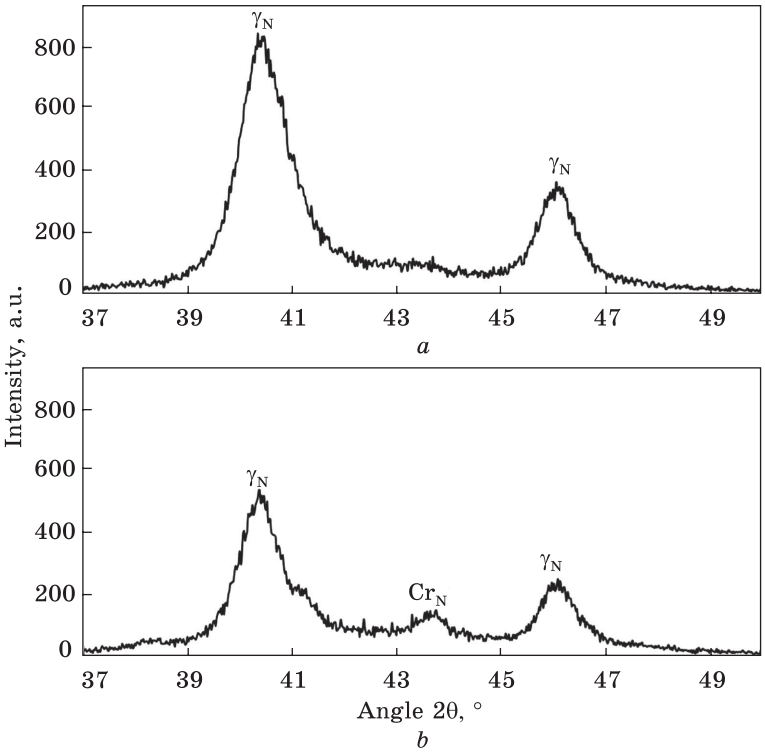

Fig. 22. XRD patterns of surface composition on AISI 304 austenitic steel nitrided in 10% N_2–90% H_2 (*a*) and 70% N_2–30% H_2 (*b*) [76]

The x-ray diffractograms obtained for the two extreme cases, show that gas mixture containing 10% N_2 (mixture No. 1) does not change significantly of nitride layer's structure. The obtained nitrided composition consists only of the γ_N-phase (Fig. 22, *a*). At the same time, a certain denitriding of the γ_N-phase with the CrN precipitation is observed when nitrogen content increases up to 70% (mixture No. 4) (Fig. 22, *b*).

Known work [75] on the study of tribological and corrosion resistance of plasma nitrided AISI 316 austenitic stainless steel influenced by gas composition. The study was carried out on samples measuring 20×20 mm and 3 mm thick. Before nitriding, the samples were grounded with SiC paper with a grain size of 600, 1000, 1200, and 2500. After that, the samples were polished with Al_2O_3 paste with a grain of 1 μm. Directly before nitriding, the samples were subjected to ion sputtering at a temperature of 673 K in an Ar:H_2 environment with concentration of 3:1 at a gas pressure in the reactor of 25 Pa for 30 min. The plasma nitriding parameters are listed in Table 5.

The experimentally obtained results show the smallest thickness of the nitrided layer (2 μm) was obtained during nitriding in a 100% N_2

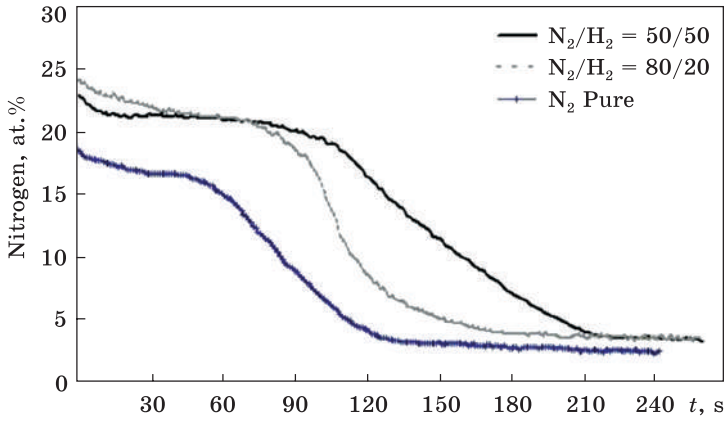

Fig. 23. Profiles of nitrogen content in AISI 316 steel samples nitrided at different gas compositions [77]

Table 5. **Plasma nitriding parameters [77]**

Sample code	Discharge voltage, V	Temperature, K	Gas pressure, Pa	Gas mixture, $N_2:H_2$ (vol.%)	Treatment time, h
StN1	600	723	80	Pure N_2	20
StN2	600	723	100	80:20	20
StN3	600	723	160	50:50	24

Table 6. **Results of corrosion tests of AISI 316 steel samples [77]**

Sample	E_{corr}, mV	i_{corr}, μA/cm^2	E_{pitt}, mV
Untreated	–440	≈25	≈+105
StN1	–409	≈51	≈+442
StN2	–375	≈40	≈+507
StN3	–395	≈18	≈+840

environment. Plasma nitriding in a mixture of $N_2:H_2$ 80:20 provided a slightly larger modified layer thickness at the level of 3.2 ± 0.1 μm. While treating in a gas mixture of $N_2:H_2$ 50:50 made it possible to obtain of modified layer thickness of 4.3 ± 0.1 μm. The nitrogen concentration profiles along the depth of samples nitrided in the different gas mixtures are shown in Fig. 23.

The obtained curves show, that the N_2 concentration on the nitrided in pure nitrogen samples surface does not exceed 18%. Instead, the addition of hydrogen to the gas mixture provided nitrogen concentration on the treated surface at the level of 22% and 24% for mixtures with 50% and 80% of H_2, respectively. The authors note the increase in the nitrided layer thickness with the addition of hydrogen to a gas composition is due to the rise in ionized nitrogen concentration in plasma as a result of secondary electron emission from the cathode. This leads, in

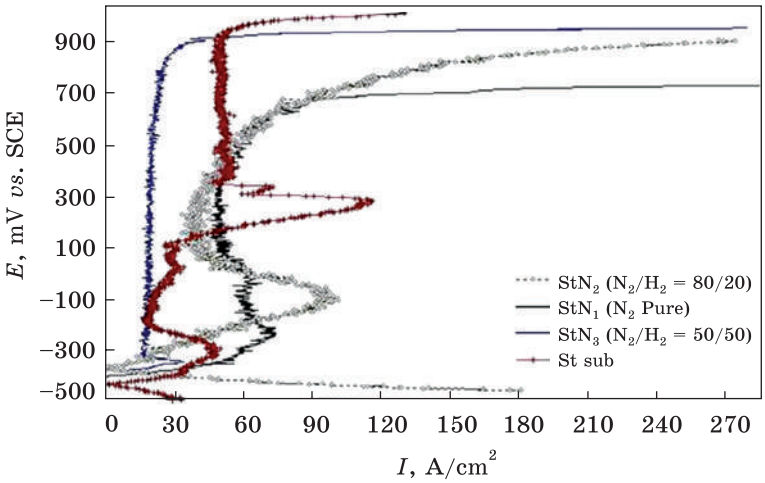

Fig. 24. Polarization curves of corrosion tests of AISI 316 steel samples [77]

turn, to a corresponding increase in the nitrogen concentration on the treated surface and its diffusion into the nitrided layer.

The polarization curves of corrosion tests of AISI 316 steel samples plasma nitrided in different gas mixtures compared with untreated samples are shown in Fig. 24. Corrosion tests of samples were carried out in 1% of H_2SO_4 solution. Table 6 shows the corrosion potential (E_{corr}), current density of anodic reactions (i_{corr}) and pitting potential (E_{pitt}) obtained as a result of corrosion tests.

Analysing the obtained results of corrosion tests, the authors note that all treated samples have a higher corrosion potential compared to the untreated sample, which increases with increasing of nitrogen content in the mixture. A certain deterioration of the steel protective properties, in comparison with the original sample, is observed on the StN1 sample, the polarization curve of which shows a higher current of anodic reactions. Obviously, this is due to the small thickness of the nitrided layer (2 μm), which is not able to resist the influence of an aggressive environment for a long time. However, the nitrided StN1 sample shows a higher pitting corrosion potential compared to the untreated one. As known, the more inert this potential is, the less sensitive the material to the pitting corrosion.

A steeper current increase and, accordingly, higher values of the primary passivation potential are shown by the StN2 sample. The authors attribute this to a change in the surface structure due to the appearance of the Fe_4N iron nitrides in the nitrided layer. The values of corrosion potential (E_{corr}) and pitting potential (E_{pitt}) move towards inertness after nitriding in the 80% N_2–20% H_2 mixture. However, the

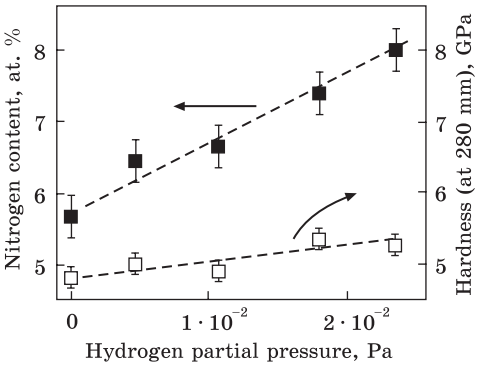

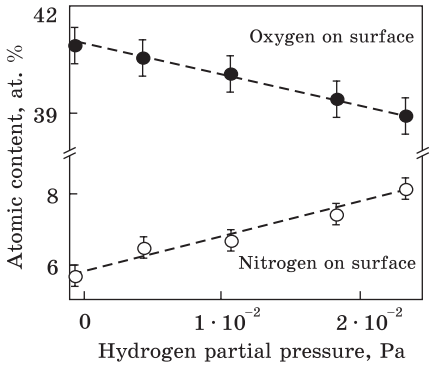

Fig. 25. The nitrogen concentration and the surface hardness of AISI 316 plasma nitrided sample depending on the hydrogen partial pressure added to the gas medium [78]

Fig. 26. The changes in the oxygen and nitrogen surface concentrations due to the variation in the hydrogen partial pressure [79]

formation of a homogeneous protective passivating layer on the surface of the StN2 sample is not observed.

Therefore, the anodic current increases along with the corrosion potential. The best corrosion performance is shown by the sample StN3, nitrided in a mixture of 50% N_2–50% H_2. Thus, for this sample, there is an increase in the potentials of E_{corr} and E_{pitt} alongside with a decrease in the corrosion currents density (i_{corr}). Additionally, a large interval between E_{corr} and E_{pitt} indicates the higher resistance to a pitting corrosion of the StN3 sample. The authors attribute the improvement of the corrosion resistance of the StN3 sample to a homogeneous γ_N-phase formation without of internal stresses and the nitrides precipitation when the hydrogen of 50% is introduced into the mixture.

As was already mentioned, the addition of hydrogen to the gas mixture facilitates the removal of natural oxides layer from the treated surface, promoting the free nitrogen penetration into the sample. Thus, in Fig. 25, a graph of nitrogen concentration and the hardness of AISI 316 steel nitrided surface as a function of the hydrogen partial pressure in the gas mixture obtained by the authors of Ref. [78] is shown.

The positive effect of hydrogen the authors associated, at first place, with an increase in the concentration of atomic nitrogen ions due to the intensification of ion–electron emission from the cathode surface [80]. Secondly, the formation of easily desorbed from the treated surface water molecules because of hydrogen–oxygen interactions. As a result, the surface concentration of oxygen goes down with an increase in the number of nitrogen atoms adsorption sites on the treated surface (Fig. 26). The latter is also results in the surface microhardness increasing.

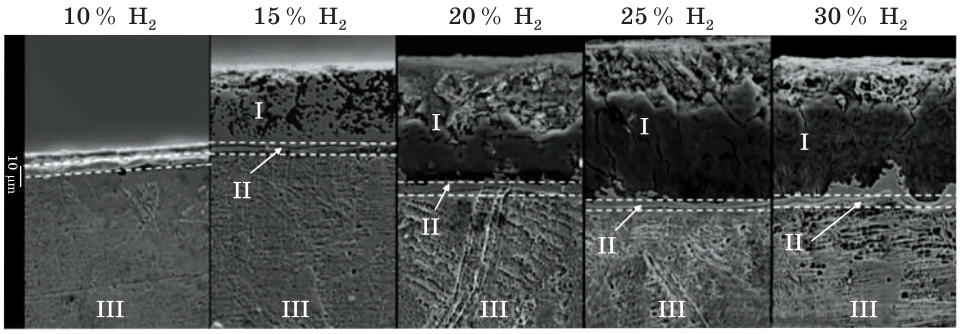

Fig. 27. The microstructure of AISI 321 steel after plasma nitriding in glow discharge with the different hydrogen content in the gas mixture [81]

Table 7. **Composition of the working gas mixture [81]**

No. of experiment	Gas mixture composition	No. of experiment	Gas mixture composition
1	60% Ar + 30% N_2 + 10% H_2	4	45% Ar + 30% N_2 + 25% H_2
2	55% Ar + 30% N_2 + 15% H_2	5	40% Ar + 30% N_2 + 30% H_2
3	50% Ar + 30% N_2 + 20% H_2		

Thus, the authors of Ref. [78] concluded that the hydrogen introduction to the gas mixture intensifies the plasma nitriding of metals with the stable oxides including stainless steels.

At the same time, the authors of Ref. [81], emphasize that an excessive increase in the H_2 in the reactor affects negatively the nitriding efficiency during the plasma nitriding of AISI 321 steel (Cr 18%, Ni 10%, Ti ≤ 1%). On the contrary, its excessive content in the working chamber inevitably leads to undesirable diffusional saturation of modified layer with H_2 resulted in the various defects (cracks, pores, *etc.*) appearance. Experiments were carried out in a 3 component N_2:H_2:Ar plasma at a nitriding temperature of 550 °C for 6 hours. The gas pressure in the working chamber was 150 Pa. The composition of the studied environments is shown in Table 7.

In Figure 27, the optical microscopy images of AISI 321 after plasma nitriding in a mixture with the different hydrogen content are given. The authors distinguish the presence of three zones in the nitrided surface layer: *I* — zone of internal nitriding; *II* — transition (diffusion) zone; *III* — base (metal matrix).

The authors report that an increase in the hydrogen content in the gas composition from 20 to 30% leads to formation of nitrided layer structural defects because of hydrogen diffusion saturation. It should be mentioned that the high-temperature treatment (about 550 °C) was applied here. As it has already been shown, this threatens the harmful

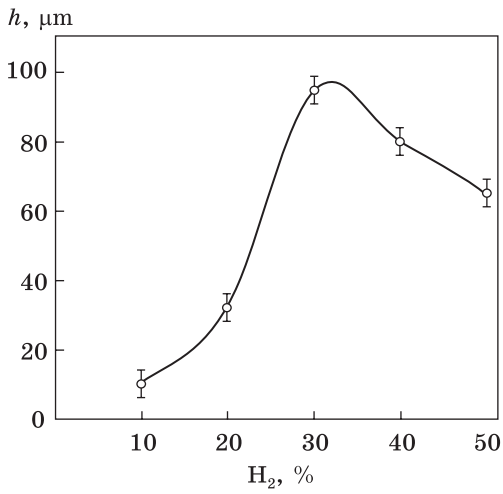

Fig. 28. Thickness of the nitrided layer on AISI 321 steel *vs.* the hydrogen content in the gas mixture [81]

Cr_xN precipitation for austenitic stainless steel. The latter, apparently, is observed by the author on the obtained images in form of dark spots in the nitriding area. Chemical analysis of AISI 321 steel surface layer plasma nitrided in a gas mixture with 25% H_2 showed an excessively high concentration of Cr at the level of 77%. This indicates high chromium diffusion on the surface of the samples. At the same time, the concentration of nitrogen in this area does not exceed 11% [81].

The intensity of nitrogen diffusion in AISI 321 steel during plasma nitriding was estimated by the growth rate of the hardened layer. The dependence of the nitrided layer thickness on the percentage of hydrogen in the gas mixture is shown in Fig. 28.

The significant intensification of treated surface diffusion saturation with atomic nitrogen when the hydrogen content in the working gas mixture increases from 10% to 20% was observed. This is evidenced by the rapid increase in the thickness of the hardened layer from 7 to 95 μm. At the same time, the surface hardness increased from 350 to 1100 HV_{100}. The further increase in the hydrogen content up to 30% leads to a slower growth of nitrided layer thickness. So, the thickness of such layer was not exceeded of 65 μm. However, a slight increase in surface hardness up to 1200 HV_{100} is noted. According to the authors, the decrease in the plasma nitriding efficiency under such conditions is caused mainly by a reduction in the cathode and reverse sputtering intensity due to decrease in Ar content in the gas mixture from 60% to 40%. As is known, the simultaneous flow of cathode and reverse cathode sputtering affect significantly the structure of the hardened layer. Depending on the nature of these processes, it is possible to obtain the modified layer consisting either with or without the nitrides phase [82]. As shown in Ref. [10], the presence of hydrogen in the gas mixture facilitates the single-phase nitrides formation of γ′-phase (Fe_4N) and the ε-phase ($Fe_{2-3}N$). These two phases also have a significant strengthening effect with a nitrogen content of 6 to 17%. Thus, the authors single out the 55%Ar–30%N_2–15%H_2 as the optimal working gas mixture, which ensures a high growth rate of the nitrided layer without

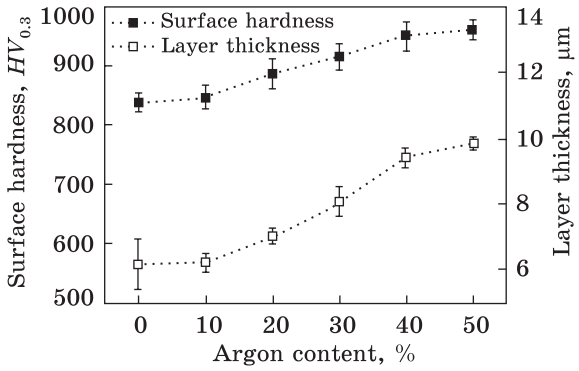

Fig. 29. Dependences of the nitrided layer thickness and hardness after nitriding of AISI 420 steel at a temperature of 350 °C for 6 hours at a gas pressure of 400 Pa [84]

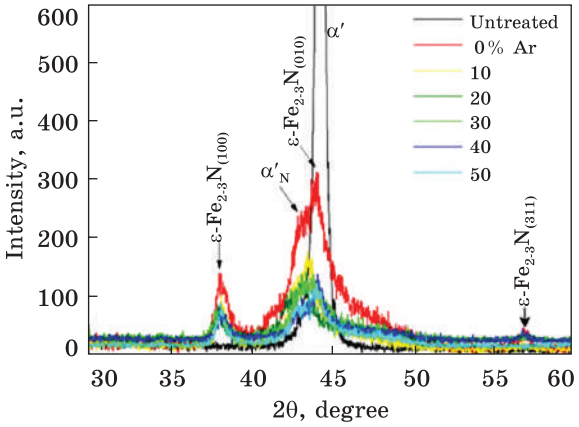

Fig. 30. X-ray diffraction patterns of AISI 420 nitrided samples at a temperature of 350 °C for 6 hours at a gas pressure of 400 Pa with different argon content in the gas mixture [84]

any structural and phase inhomogeneity.

At the same time, in Ref. [83] the comparison of the effect of hydrogen-containing gas mixture with the hydrogen-free on the plasma nitriding rate is given. The results show that the nitriding rate constant in the mixture of 75% N_2–25% Ar is much higher than those one containing of 75% N_2 — 25% H_2. The authors of Ref. [65] also observe the intensification in the modified layer growth during plasma nitriding in a N_2:Ar gas mixture, but the depth of nitrogen penetration was much lo-wer than in N_2:H_2. All treated samples mainly made up of ε and γ′-phases of iron nitrides. The ε-phase percentage was low when using a gas mixture of 10% N_2 + 90% Ar.

The authors of Ref. [84] also reported an increase in the hardened layer thickness on AISI 420 steel from 6 to 10 μm with the rise in the Ar percentage in the gas composition from 10 to 50%. The hardness of the nitrided surface also increased from 850 *HV* to 960 *HV*. The research was carried out at a nitriding temperature of 350 °C for 6 hours at a gas pressure of 400 Pa. Dependences of the nitrided layer thickness and its hardness on the Ar percentage in the working gas mixture are shown in Fig. 29.

Analysing the obtained results, the authors emphasize the essential role of argon in the molecular nitrogen dissociation with the formation of its reactive radicals. Thus, an increase in the argon percentage in the gas mixture leads to an increase in the number of reactive atomic nitrogen ions. The XRD patterns of nitrided samples with different argon

content are shown in Fig. 30. The obtained results show that the surface layer nitrided under such conditions consists mainly of ε-phase of iron nitrides $Fe_{2-3}N$ and α'_N-phase of expanded martensite. Note that martensitic α′-phase of Fe–N can transform (at a tempering of 120–150 °C) into the martensite α′-$Fe_{16}N_2$ known as a phase with extraordinary magnetic properties, including the largest saturation magnetization [85–87].

5. Conclusions

In order to increase the mechanical and tribological properties of stainless steels, methods of surface strengthening based on diffusional thermochemical treatment have shown their high efficiency. Particularly, glow discharge plasma nitriding has become a good alternative to a gas nitriding for strengthening of stainless steel surfaces. It is shown that the plasma nitriding efficiency is determined by the concentration of active particles on the treated surface and the rate of diffusion processes in the samples volume, which increase along with the nitriding temperature.

At the same time, the prevalent majority of researchers indicate that for preventing of harmful Cr_xN-phase precipitation on the surfaces of stainless steel, a low-temperature plasma nitriding (≤450 °C) should be applied. Under such conditions, the formation of a homogeneous nitrided layer with the expanded by nitrogen phase of ferrite (α_N), martensite (α'_N) or austenite (γ_N) with a high nitrogen concentration is formed. However, while low-temperature plasma nitriding, in order to obtain a thick enough nitrogen diffusion-saturated layer, the long-time treatment should be provided. This leads to a dramatically decrease in the efficiency of glow-discharge plasma nitriding of stainless steels.

It is shown the way of intensification of stainless steels low-temperature plasma nitriding by means of verification of the working gas composition and its pressure in the reactor. The increase in the ion nitriding efficiency with the rising of working gas pressure in the range from 130 to 400 Pa was established. Such an increase resulted in the rising of nitrided layer thickness and its hardness of 8 μm up to 18 μm and 700 *HV* up to 1500 *HV*, respectively. A further increase in a gas pressure leads to some reduction in the modified layer thickness mainly because of the decrease in the free path length of atomic nitrogen ions.

The significant influence of the gas composition in the reactor on the structure, properties and a growth rate of the modified layer on the surface of stainless steels while nitriding in a glow discharge plasma is given. The low efficiency of stainless steel ion nitriding in a pure nitrogen (100% N_2) environment was established. In turn, an increase in the nitrogen content in the nitrogen-hydrogen gas mixture from 10% to

50% leads to the growth of the modified layer thickness on the stainless steel surfaces. However, the deterioration of their corrosion performance due to the chromium nitrides precipitation when the nitrogen content goes up from 30 to 80% is observed.

At the same time, the undesirable diffusion saturation of nitrided steel surfaces with hydrogen is observed when the H_2 content increases from 20 to 30% in N_2:H_2 plasma. The latter resulted in the formation of structural inhomogeneity (pores and cracks) on the plasma nitrided surfaces. Therefore, the three-component gas composition containing of 55%Ar — 30%N_2 — 15%H_2 can be singled out as the optimal, providing the highest mechanical and tribological properties of ion nitrided stainless steel surface.

REFERENCES

1. K.H. Lo, C.H. Shek, and J.K.L. Lai, Recent developments in stainless steels, *Mater. Sci. Eng. R*, **65**, Nos. 4–6: 39–104 (2009); https://doi.org/10.1016/j.mser.2009.03.001
2. N.R. Baddoo, Stainless steel in construction: A review of research, applications, challenges and opportunities, *J. Constr. Steel Res.*, **64**, No. 11: 1199–1206 (2008); https://doi.org/10.1016/j.jcsr.2008.07.011
3. K. Ram Mohan Rao, Corinne Nouveau, and Kalimi Trinadh, Low-temperature plasma nitriding of martensitic stainless steel, *Trans. Indian Inst. Met.*, **73**: 1695–1699 (2020); https://doi.org/10.1007/s12666-020-02013-8
4. H. Dong, S-phase surface engineering of Fe–Cr, Co–Cr and Ni–Cr alloys, *Int. Mater. Rev.*, **55**, No. 2: 65–98 (2010); https://doi.org/10.1179/095066009X12572530170589
5. M.G. Bolotov and I.O. Prybytko, Application of glow discharge plasma for cleaning (activation) and modification of metal surfaces while welding, brazing, and coating deposition, *Prog. Phys. Met.*, **22**, No. 1: 103–128 (2021); https://doi.org/10.15407/ufm.22.01.103
6. A.A. Babad–Zahryapin and G.D. Kuznetsov, *Radiatsionno-Stimuliruemaya Khimiko-Termiceskaya Obrabotka* [Radiational Stimulated Thermochemical Treatment] (Moskva: Ehnergoizdat: 1982) (in Russian).
7. R.P. Cardoso, S.F. Brunatto, C.J. Scheuer, and S.F. Brunatto, Low-temperature nitriding kinetics, *Encyclopedia of Iron, Steel, and Their Alloys* (1st Edition) (New York: Taylor & Francis Group: 2016); https://doi.org/10.1081/E-EISA-120051669
8. S.V. Pogorelov, I.V. Krasovskyi, V.A. Timaniuk, and N.G. Kokodii, Investigation of a glow discharge with a coaxial hollow cathode, *East Eur. J. Phys.*, **2**: 85–90 (2022); https://doi.org/10.26565/2312-4334-2022-2-10
9. T. Borowski, B. Adamczyk-Ciesrlak, A. Brojanowska, K. Kulikowski, and T. Wierzchon, Surface modification of austenitic steel by various glow-discharge nitriding methods, *Mater. Sci.*, **21**: 376–381 (2015); https://doi.org/10.5755/j01.ms.21.3.7404
10. Yu.M. Lahtin and Ya.D. Kogan, *Azotirovanie Stali* [Nitriding of Steel] (Moskva: Mashinostroyenie: 1976) (in Russian).

11. B.M. Kramer, Requirements for wear-resistant coatings, *Thin Solid Films*, **108**, No. 2: 117–125 (1983);
https://doi.org/10.1016/0040-6090(83)90497-2
12. R.W. Hoffnau, Stress distributions and thin film mechanical properties, *Surface and Interface Analysis*, **3**, No. 1: 62–66 (1981);
https://doi.org/10.1002/sia.740030113
13. Yu.M. Lahtin and B.N. Arzamasov, *Khimiko-Termicheskaya Obrabotka Metallov* [Thermochemical Treatment of Metals] (Moskva: Metallurgiya: 1985) (in Russian).
14. Rodrigo P. Cardoso, Marcio Mafra, and Silvio F. Brunatto, Low-temperature thermochemical treatments of stainless steels — an introduction, *Plasma Science and Technology. Progress in Physical States and Chemical Reactions* (Ed. Tetsu Mieno) (IntechOpen: 2016);
https://doi.org/10.5772/61989
15. B.N. Arzamasov, *Khimiko-Termicheskaya Obrabotka Metallov v Aktivizirovannykh Gazovykh Sredakh* [Thermochemical Treatment of Metals in the Active Gas Medium] (Moskva: Mashinostroyenie: 1979) (in Russian).
16. T.L. Christiansen, T.S. Hummelshшj, and M.A.J. Somers, Expanded austenite, crystallography and residual stress, *Surf. Eng.*, **26**, 242–247 (2010);
https://doi.org/10.1179/026708410X12506870724316
17. Z. Balogh and G. Schmitz, Diffusion in Metals and Alloys, *Phys. Metallurgy* (5th Edition) (Elsevier: 2014), p. 387–559;
https://doi.org/10.1016/B978-0-444-53770-6.00005-8
18. Kai Wang, Xin Chen, Siyi Huang, Xingyu Chen, Zumin Wang, and Yuan Huang, Diffusion behavior determined by the new n-body potential in highly immiscible W/Cu system through molecular dynamics simulations, *J. Mater. Res. Technol.*, **24**: 3731–3745 (2023);
https://doi.org/10.1016/j.jmrt.2023.04.068
19. R.E. Cunningham and R.J.J. Williams, Constitutive equations of diffusion and wall effects, *Diffusion in Gases and Porous Media* (Boston, MA: Springer: 1980);
https://doi.org/10.1007/978-1-4757-4983-0_4
20. Y. Syrovatko and Y. Shtapenko, Determination of activation energy of surface diffusion based on thermal oscillations of atoms, *Physics and Chemistry of Solid State*, **22**, No. 3: 522–528 (2021);
https://doi.org/10.15330/pcss.22.3.522-528
21. A.A. Babad-Zahryapin and G.D. Kuznecov, *Khimiko-Termicheskaya Obrabotka v Tleyushchem Razriade* [Thermochemical Treatment in a Glow Discharge] (Moskva: Atomizdat: 1975) (in Russian).
22. A.V. Belyj, V.A. Kukareko, I.Yu. Tarasevich, S.K. Shih, and I.V. Boyarenko, Vliyanie Plotnosti Ionnogo Toka na Strukturnye Parametry i Svojstva Poverhnostnyh Sloev Hromosoderzhashih Splavov Zheleza, Modificirovannyh Ionami Azota [The Impact of Ion Current Density on The Structural Features And Properties of Surface Layer of Chromium Iron Alloys Modified by Nitrogen Atoms], *Fizika i Khimiya Obrabotki Materialov*, No. 4: 11–17 (2000) (in Russian).
23. V.A. Moskvina, E.G. Astafurova, N.K. Galchenko, E.V. Melnikov, G.G. Mayer, V.A. Bataev, and I.A. Bataev, The effect of severe plastic deformation by high pressure torsion on structure and phase composition of high-nitrogen austenitic steel, *AIP Conf. Proc.*, **1683**, No. 1: 020153 (2015);
https://doi.org/10.1063/1.4932843
24. W.P. Tong, C.Z. Liu, W. Wang, N.R. Tao, Z.B. Wang, L. Zuo, and J.C. He, Gaseous nitriding of iron with a nanostructured surface layer, *Scripta Mater.*,

57, No. 6: 533–536 (2007);
https://doi.org/10.1016/j.scriptamat.2007.05.017
25. A.P. Tschiptschin, A.S. Nishikawa, L.B. Varela, and C.E. Pinedo, Thermal stability of expanded austenite formed on a DC plasma nitrided 316L austenitic stainless steel, *Thin Solid Films*, **644**: 156–165 (2017);
https://doi.org/10.1016/j.tsf.2017.06.065
26. A. Bekmurzayeva, W.J. Duncanson, H.S. Azevedo, and D. Kanayeva, Surface modification of stainless steel for biomedical applications: revisiting a century-old material, *Mater. Sci. Eng.*, **93**: 1073–1089 (2018);
https://doi.org/10.1016/j.msec.2018.08.049
27. T. Frączek, R. Prusak, M. Ogyrek, and Z. Skuza, Nitriding of 316L steel in a glow discharge plasma, *Materials*, **15**: 3081 (2022);
https://doi.org/10.3390/ma15093081
28. F. Borgioli, E. Galvanetto, and T. Bacci, Low temperature nitriding of AISI 300 and 200 series austenitic stainless steels, *Vacuum*, **127**: 51–60 (2016);
https://doi.org/10.1016/j.vacuum.2016.02.009
29. K. Lin, X. Li, H. Dong, P. Guo, and D. Gu, Nitrogen mass transfer and surface layer formation during the active screen plasma nitriding of austenitic stainless steels, *Vacuum*, **148**: 224–229 (2018);
https://doi.org/10.1016/j.vacuum.2017.11.022
30. V. Moskvina, G. Maier, E. Melnikov, S. Astafurov, E. Zagibalova, M. Panchenko, K. Reunova, A. Nikolaev, K. Ramazanov, and E. Astafurova, The effect of thin surface layer of nitrogen-expanded austenite on bulk γ–α' phase transformation in low-temperature deformation of 316L stainless steel, *Mater. Lett.*, **304**: 130676 (2021);
https://doi.org/10.1016/j.matlet.2021.130676
31. Elieser Arajo, Rafael Bandeira, Marcos Manfrinato, Jeferson Moreto, and Roger Borges, Effect of ionic plasma nitriding process on the corrosion and micro-abrasive wear behavior of AISI 316L austenitic and AISI 470 super-ferritic stainless steels, *J. Mater. Res. Technol.*, **8**, No. 2: 2180–2191 (2019);
https://doi.org/10.1016/j.jmrt.2019.02.006.
32. G.E. Totten, L.C. Casteletti, F.A.P. Fernandes, and J. Gallego, Microstructural characterization of layers produced by plasma nitriding on austenitic and super-austenitic stainless steel grades, *J. ASTM Int.*, **9**, No. 2: 1–11 (2011);
https://doi.org/10.1520/JAI103564
33. F. Borgioli, A. Fossati, E. Galvanetto, and T. Bacci, Glow-discharge nitriding of AISI-316L austenitic stainless steel: influence of treatment temperature. *Surf. Coat. Technol.*, **200**: 2474–2480 (2005);
https://doi.org/10.1016/j.surfcoat.2004.07.110
34. M. Esfandiari and H. Dong, Improving the surface properties of A286 precipitation-hardening stainless steel by low-temperature plasma nitriding, *Surf. Coat. Technol.*, **201**: 6189–6196 (2007);
https://doi.org/10.1016/j.surfcoat.2006.11.013
35. J.F.V. Lima, C.J. Scheuer, S.F. Brunatto, and R.P. Cardoso, Kinetics of the UNS S32750 super duplex stainless steel low-temperature plasma nitriding, *Mater. Res.*, **25**: e20210463 (2022);
https://doi.org/10.1590/1980-5373-mr-2021-0463
36. X, Li, W. Dou, L. Tian, and H. Dong, Combating the tribo-corrosion of LDX2404 lean duplex stainless steel by low temperature plasma nitriding. *Lubricants*, **6**, No. 4: 93 (2018);
https://doi.org/10.3390/lubricants6040093

37. A.P. Tschiptschin, L.B. Varela, C.E. Pinedo, X.Y. Li, and H. Dong, Development and microstructure characterization of single and duplex nitriding of UNS S31803 duplex stainless steel, *Surf. Coat. Technol.*, **327**: 83–92 (2017); https://doi.org/10.1016/j.surfcoat.2017.08.018
38. A. Fossati, F. Borgioli, E. Galvanetto, and T. Bacci, Glow-discharge nitriding of AISI-316L 170 austenitic stainless steel: influence of treatment time. *Surf. Coat. Technol.*, **200**: 3511–3517 (2006); https://doi.org/10.1016/j.surfcoat.2004.10.122
39. Carlos E. Pinedo and Waldemar A. Monteiro, On the kinetics of plasma nitriding a martensitic stainless steel type AISI 420, *Surf. Coat. Technol.*, **179**, Nos. 2–3: 119–123 (2004); https://doi.org/10.1016/S0257-8972(03)00853-3
40. M. Lepicka and G. Małgorzata, Effect of heat treatment and plasma nitriding on corrosion resistance of 440B martensitic stainless steel, *Acta Mechanica et Automatica*, **7**, No. 3: 156–159 (2014); https://doi.org/10.2478/ama-2014-0028
41. L. Ferreira, S.F. Brunatto, and R.P. Cardoso, Martensitic stainless steels low-temperature nitriding: dependence of substrate composition, *Mater. Res.*, **18**, No. 3: 622–627 (2015); https://doi.org/10.1590/1516-1439.015215
42. Hongyu Shen and Liang Wang, Mechanism and properties of plasma nitriding AISI 420 stainless steel at low temperature and anodic (ground) potential, *Surf. Coat. Technol.*, **403**: 126390 (2020); https://doi.org/10.1016/j.surfcoat.2020.126390
43. C.J. Scheuer, R.P. Cardoso, M. Mafra, and S.F. Brunatto, AISI 420 martensitic stainless steel low-temperature plasma assisted carburizing kinetics. *Surf Coat Tech.*, **214**: 30–37 (2013); https://doi.org/10.1016/j.surfcoat.2012.10.060
44. C.J. Scheuer, A.C. Gralak, F.I. Zanetti, T.F. Amaral, R. Pereira, S.F. Brunatto, and R.P. Cardoso, Effect of plasma nitriding parameters on surface properties of low-temperature nitrided AISI 420 martensitic stainless steel, *Conference Proc.: 68th ABM International Congress* (2013), p. 3733–3743.
45. Y. Li, Y. He, J. Xiu, W. Wang, Y. Zhu, and B. Hu, Wear and corrosion properties of AISI 420 martensitic stainless steel treated by active screen plasma nitriding, *Surf. Coat. Technol.*, **329**: 184–192 (2017); https://doi.org/10.1016/j.surfcoat.2017.09.021
46. D. Kusmic, O. Cech, and L. Klakurkov, Corrosion resistance of ferritic stainless steel X12Cr13 after application of low-temperature and high-temperature plasma nitriding, *Manufacturing Technol.*, **21**, No. 1: 98–104 (2021); https://doi.org/10.21062/mft.2021.013
47. S.Y. Sirin and E. Kaluc, Structural surface characterization of ion nitrided AISI 4340 steel, *Mater. Design*, **36**: 741–747 (2012); https://doi.org/10.1016/j.matdes.2011.12.025
48. W. Tuckart, E. Forlerer, and L. Iurman, Delayed cracking in plasma nitriding of AISI 420 stainless steel, *Surf. Coat. Technol.*, **202**: 199–202 (2007); https://doi.org/10.1016/j.surfcoat.2007.04.107
49. A.N. Allenstein, C.M. Lepienski, A.J.A. Buschinelli, and S.F. Brunatto, Plasma nitriding using high H2 content gas mixtures for a cavitation erosion resistant steel, *Appl. Surf. Sci.*, **277**: 15–24 (2013); https://doi.org/10.1016/j.apsusc.2013.03.055
50. O. Comakli, A.F. Yetim, B. Karaca, and A. Celik, Effect of gas mixture on tribological performance of plasma nitrided grey cast iron under dry and lubricated

conditions, *Mater. Res. Express*, **6**, No. 5: (2019); https://doi.org/10.1088/2053-1591/ab012b
51. Li Zhong and Xi Han, Influence of Hydrogen on the Plasmas Nitriding Process of 35CrMo Steel, *Advanced Mater. Res.*, **295–297**: 1004–1009 (2011); https://doi.org/10.4028/www.scientific.net/AMR.295-297.1004
52. K. Ram Mohan Rao, Kalimi Trinadh, and Corinne Nouveau, Elevated temperature plasma nitriding and effects on electrochemical properties of steel, *Mater. Today: Proc.*, **19**, No. 2: 867–869 (2019); https://doi.org/ff10.1016/j.matpr.2019.08.227ff
53. M.K. Sharma, B.K. Saikia, A. Phukan and B. Ganguli, Plasma nitriding of austenitic stainless steel in N_2 and N_2–H_2 dc pulsed discharge. *Surf. Coat. Technol.*, **201**: 2407–2413 (2006); https://doi.org/10.1016/j.surfcoat.2006.04.006
54. Liang Wang, Shijun Ji, and Juncai Sun, Effect of nitriding time on the nitrided layer of AISI-304 austenitic stainless steel. *Surf. Coat. Technol.*, **200**: 5067–5070 (2006); https://doi.org/10.1016/j.surfcoat.2005.05.036
55. Liang Wang, Yang Li, and Xuemin Wu, Plasma nitriding of low alloy steels at floating and cathodic potentials, *Appl. Surf. Sci.*, **254**, No. 20: 6595–6600 (2008); https://doi.org/10.1016/j.apsusc.2008.04.027
56. J. Baranowska, Characteristic of the nitride layers on the stainless steel at low temperature, *Surf. Coat. Technol.*, **180–181**: 145–149 (2004); https://doi.org/10.1016/j.surfcoat.2003.10.056
57. Xu Xiaolei, Wang Liang, Yu Zhiwei, and Hei Zukun, A comparative study on microstructure of the plasma-nitrided layers on austenitic stainless steel and pure Fe, *Surf. Coat. Technol.*, **192**, Nos. 2–3: 220–224 (2005); https://doi.org/10.1016/j.surfcoat.2004.04.085
58. B.N. Arzamasov, A.G. Bratuhin, Yu.S. Eliseev, and T.A. Panajoti, *Ionnaya Khimiko-Termicheskaya Obrabotka Splavov* [Ion Thermochemical Treatment of Alloys] (Moskva: Izd. MGTU im. Baumana: 1999) (in Russian).
59. G.P. Bolotov, M.G. Bolotov, and S.M. Yushchenko, Stabilization of a high-current glow discharge under the welding conditions, *2018 IEEE 38th Int. Conf. Electronics and Nanotechnology (ELNANO) (24–26 April 2018, Kyiv)* (Kyiv: 2018); https://doi.org/10.1109/ELNANO.2018.8477494
60. G.P. Bolotov, M.G. Bolotov, and S.A. Stepenko, The ways of stabilization of high-current glow discharge in welding, *2018 IEEE 3rd Int. Conf. Intelligent Energy and Power Systems (IEPS) (10–14 September 2018, Kharkiv)* (Kharkiv: 2018); https://doi.org/10.1109/IEPS.2018.8559580
61. M.G. Bolotov and G.P. Bolotov, Elimination of electric arc stabilization in precision welding with high-current dc glow discharge, *2019 IEEE 39th Int. Conf. Electronics and Nanotechnology (ELNANO-2019) (16–18 April 2019, Kyiv)* (Kyiv: 2019); https://doi.org/10.1109/ELNANO.2019.8783845
62. M.G. Bolotov and G.P. Bolotov, Criterial definition of the limits of glow discharge energy stability in welding, *2019 IEEE 2nd Ukraine Conf. Electrical and Computer Engineering (UKRCON) (02–06 July 2019, Lviv)* (Lviv: 2019); https://doi.org/10.1109/UKRCON.2019.8879992
63. M. Bolotov, G. Bolotov, S. Stepenko, and P. Ihnatenko, Impact of the samples' surface state on the glow discharge stability in the metals' treatment and welding processes, *Appl. Sci.*, **11**, No. 4: 1765 (2021); https://doi.org/10.3390/app11041765

64. Yu.P. Raizer, *Fizika Gazovogo Razryada* [Gas Discharge Physics] (Moskva: Nauka: 1987) (in Russian).
65. E.V. Berlin, N.N. Koval, and L.A. Sejdman, *Plazmennaya himiko-termicheskaya obrabotka poverhnosti stalnyh detalej* [Plasma thermochemical treatment of steel samples surfaces] (Moskva: Tekhnosfera: 2012) (in Russian).
66. T.A. Panajoti, Sozdanie maksimalnoj nasyshayushej sposobnosti gazovoj sredy pri ionnom azotirovanii splavov. [Creation of maximum saturating ability of a gas medium during ion nitride of steels], *Fizika i Khimiya Obrabotki Materialov*, **4**: 70–78 (2003).
67. F. Borgioli, A. Fossati, E. Galvanetto, T. Bacci, and G. Pradelli, Glow discharge nitriding of AISI-316L austenitic stainless steel: Influence of treatment pressure. *Surf. Coat. Technol.*, **200**, No. 11: 5505–5513 (2006); https://doi.org/10.1016/j.surfcoat.2005.07.073
68. S. Wang, W. Cai, J. Li, W. Wei, and J. Hu, A novel rapid D.C. plasma nitriding at low gas pressure for 304 austenitic stainless steel, *Mater. Lett.*, **105**: 47–49 (2013); https://doi.org/10.1016/j.matlet.2013.04.031
69. S. Lu, X. Zhao, S. Wang, J. Li, W. Wei, and J. Hu, Performance enhancement by plasma nitriding at low gas pressure for 304 austenitic stainless steel. *Vacuum*, **145**: 334–339 (2017); https://doi.org/10.1016/j.vacuum.2017.09.020
70. F. Borgioli, E. Galvanetto, and T. Bacci, Influence of surface morphology and roughness on water wetting properties of low temperature nitrided austenitic stainless steels, *Mater. Charact.*, **95**: 278–284 (2014); https://doi.org/10.1016/j.matchar.2014.07.006
71. S. Guruvenket, D. Li, J.E. Klemberg-Sapieha, L. Martinu, and J. Szpunar, Mechanical and tribological properties of duplex treated TiN, nc-TiN/a-SiN_x and nc-TiCN/a-SiCN coatings deposited on 410 low alloy stainless steel, *Surf. Coat. Technol.*, **203**, No. 19: 2905–2911 (2009); https://doi.org/10.1016/j.surfcoat.2009.03.009
72. J-D. Kamminga, D. Doerwald, M. Schreurs, and G.C.A.M. Janssen, Industrial feasibility of the nitrocoat process, *Surf. Coat. Technol.*, **200**, No. 5: 1837–1841 (2005); https://doi.org/10.1016/j.surfcoat.2005.08.008
73. K.G. Kostov, M. Ueda, M. Lepiensky, P.C. Soares Jr., G.F. Gomes, M.M. Silva, and H. Reuther, Surface modification of metal alloys by plasma immersion ion implantation and subsequent plasma nitriding, *Surf. Coat. Technol.*, **186**, No. 1: 204–208 (2004); https://doi.org/10.1016/j.surfcoat.2004.04.027
74. Linda Gil, Sonia Bruhl, Lorena Jimenez, Ovidio Leon, Rafael Guevara, and Mariana H. Staia, Corrosion performance of the plasma nitrided 316L stainless steel, *Surf. Coat. Technol.*, **201**, No. 7: 4424–4429 (2006); https://doi.org/10.1016/j.surfcoat.2006.08.081
75. M. Lepicka and M. Grądzka-Dahlke, Effect of plasma nitriding process conditions on corrosion resistance of 440B martensitic stainless steel, *Acta Mechanica et Automatica*, **8**, No. 3: 156–159 (2014); https://doi.org/10.2478/ama-2014-0028
76. A. Sitko, M. Szkodo, and M. Gazda, The influence of gas mixture in the glow-discharge nitriding process of austenitic stainless steel on characteristic of nitrided cases, *Key Eng. Mater.*, **490**: 282–287 (2012); https://doi.org/10.4028/www.scientific.net/KEM.490.282
77. Saeid Amiri and Masoud Moradshahi, Influence of different layer microstructures induced by different gas compositions on corrosion behavior of plasma ni-

trided stainless steel, *Surf. Coat. Technol.*, **201**, Nos. 16–17: 7375–7381 (2007); https://doi.org/10.1016/j.surfcoat.2007.02.006.
78. C.A. Figueroa and F. Alvarez, New pathways in plasma nitriding of metal alloys, *Surf. Coat. Technol.*, **200**: 498–501 (2005); https://doi.org/10.1016/j.surfcoat.2005.02.089
79. C.A. Figueroa, S. Weber, T. Czerwiec, and F. Alvarez, Oxygen, hydrogen, and deuterium effects on plasma nitriding of metal alloys, *Sripta Mater.*, **54**, No. 7: 1335 (2006); https://doi.org/10.1016/j.scriptamat.2005.12.013
80. M.K. Sharma, B.K. Saikia, and S. Bujarbarua, Optical emission spectroscopy of DC pulsed plasmas used for steel nitriding, *Surf. Coat. Technol.*, **203**, No. 3: 229–233 (2008); https://doi.org/10.1016/j.surfcoat.2008.08.036
81. Yu.G. Husainov, K.N. Ramazanov, R.S. Esipov, and G.B. Isyandavletova, Vliyanie vodoroda na process ionnogo azotirovaniya austenitnoi stali 12H18N10 [Influence of hydrogen on the ion nitriding process of austenitic stainless steels], *Vestnik UGATU*, **21**, No. 2: 24–29 (2017) (in Russian).
82. A.I. Yunusov, Vliyanie sostava gazovoj sredy na process ionnogo azotirovaniya martensitnoj stali 15H16K5N2MVFAB-Sh [The influence of gas mixture on the process of ion nitriding of martensitic steel 15Cr16K5N2MVFAB-Sh], *Int. J. Vestnik Nauki*, **5**, No. 62: 854–864 (in Russian).
83. P.V. Kaplun, E.B. Soroka, and A.V. Snozik, The impact of hydrogen-free ion nitriding on physicomechanical and performance characteristics of hard alloys T5K10 and T15K6, *J. Superhard. Mater.*, **40**: 384–391 (2018); https://doi.org/10.3103/S1063457618060035
84. R.P. Cardoso, C.E.M. Zarbin, C.J. Scheuer, and S.F. Brunatto, Corrosion resistance of plasma nitrided AISI 420 martensitic stainless steel: influence of the pretreatment and treatment temperature, *69 Congresso Anual da ABM – Internacional*, **69**, No. 69: 7995–8005 (2014); https://doi.org/10.5151/1516-392X-24785
85. T.M. Radchenko, O.S. Gatsenko, V.V. Lizunov, and V.A. Tatarenko, Martensitic α''-$Fe_{16}N_2$-type phase of non-stoichiometric composition: current status of research and microscopic statistical-thermodynamic model, *Prog. Phys. Met.*, **21**, No. 4: 580–618 (2020); https://doi.org/10.15407/ufm.21.04.580
86. K.H. Levchuk, T.M. Radchenko, and V.A. Tatarenko, High-temperature entropy effects in tetragonality of the ordering interstitial–substitutional solution based on body-centred tetragonal metal, *Metallofiz. Noveishie Tekhnol.*, **43**, No. 1: 1–26 (2021) (in Ukrainian); https://doi.org/10.15407/mfint.43.01.0001
87. T.M. Radchenko, O.S. Gatsenko, V.V. Lizunov, and V.A. Tatarenko, *Fundamentals of Low-Dimensional Magnets* (1st Edition) (Eds. R.K. Gupta, S.R. Mishra, and T.A. Nguyen) (Boca Raton: Taylor & Francis, CRC Press: 2022), Ch. 18, p. 343–364; https://doi.org/10.1201/9781003197492-18

Received 31.08.2023
Final version 12.02.2024

М.Г. Болотов, Г.П. Болотов, М.М. Руденко
Національний університет «Чернігівська політехніка»,
вул. Шевченка 95, 14035 Чернігів, Україна

ВПЛИВ ПАРАМЕТРІВ АЗОТУВАННЯ НА ЕВОЛЮЦІЮ ВЛАСТИВОСТЕЙ ПОВЕРХНІ НЕІРЖАВІЙНОЇ КРИЦІ, АЗОТОВАНОЇ В ПЛАЗМІ ЖЕВРІЙНОГО РОЗРЯДУ

Плазмове азотування в жеврійному розряді є відносно новим і надзвичайно перспективним методом поверхневого зміцнення криці. Йонами азотовані зразки демонструють тенденцію до більш тривалого терміну служби за сильного зносу та циклічних навантажень порівняно з традиційним газовим азотуванням. Одначе істотним недоліком плазмового хеміко-термічного оброблення є його відносно велика тривалість близько 20–30 годин. В результаті оброблення поверхні стає неефективним і занадто дорогим. Відомо, що властивості азотованого шару, його фазовий склад і швидкість росту сильно залежать від параметрів плазмового азотування (температури, часу, тиску газу, складу газової суміші тощо). Водночас залишається відкритим питання щодо вибору оптимальних режимів плазмового азотування важко азотованих неіржавійних криць, які забезпечать високу ефективність оброблення й одержання високотвердих зміцнених шарів із контрольованим структурно-фазовим складом. Встановлено, що для запобігання утворенню на поверхні неіржавійних криць виділень метастабільних фаз Cr–N, поява яких призводить до погіршення їхніх корозійних властивостей, температура оброблення має бути обмеженою: ≤450 °C. Низькотемпературне плазмове азотування забезпечує утворення однорідного азотованого шару «білої» фази з концентрацією Нітроґену в 15 ат.% і більше. Така фаза забезпечує твердість азотованої поверхні на рівні 1500 *HV*, що в 4–5 разів перевищує твердість необроблених зразків. Показано можливість інтенсифікації плазмового азотування шляхом підвищення тиску газу в реакторі в діяпазоні від 130 до 400 Па. Це забезпечує збільшення товщини азотованого шару та його твердости від ≈8 мкм до ≈18 мкм і ≈700 *HV* до ≈1500 *HV* відповідно. Значну динаміку зростання азотованого шару на поверхнях неіржавійних криць досягли шляхом визначення оптимальної 3-компонентної газової суміші із вмістом 55% Ar–30% N_2–15% H_2, яка забезпечила одержання зміцненого шару товщиною у ≈30 мкм із поверхневою твердістю у 1100 *HV*.

Ключові слова: жеврійний розряд, плазмове азотування, хеміко-термічне оброблення, йонне модифікування поверхні, корозійностійкі криці.